

# Exploratorium: a library of real time simulations for applied ODEs. Rigid body motion

Alexander Gofen

The Taylor Center, <http://TaylorCenter.org>, [alex@taylorcenter.org](mailto:alex@taylorcenter.org)

February 12, 2024

## **Abstract**

This library of simulations utilizes an advanced ODE solver called the Taylor Center capable to integrate initial value problems with high accuracy and to display solutions as real time animations in 2D and 3D stereo (viewable via red/blue glasses).

These unique graphical features and the user friendly interface provide the environment of a virtual laboratory allowing to observe the important dynamic behavior of the problems collected in the library, and to experiment modifying the initial values - as though during the real life laboratory work.

This first issue of the Exploratorium illustrates various type of motion of a rigid body.

# Preface

Terminology

Installation and running the simulations

# Rolling disk

The ODEs in the mathematical form

Method of visualization

Equations in the software

Visualizing the meaning of the angular velocities  $\dot{\theta}$ ,  $\dot{\phi}$ ,  $\dot{\psi}$

The meaning of  $\dot{\theta}$

The meaning of  $\dot{\phi}$

The meaning of  $\dot{\psi}$

Uniform motion:  $\dot{\theta}$ ,  $\dot{\phi}$ ,  $\dot{\psi}$  remain constant

The Euler Disk.

Discussion.

Examples from Dmitry Garanin [2]

# Free top; Physical setting

The ODEs in the mathematical form

The special cases; the  $\{\theta(t), \psi(t)\}$  phase portrait

Gyroscope

The phase portrait when  $I_1$  and  $I_2$  are close

Method of visualization

Equations in the software

General position cases

Rotation around  $I_1$  only

Rotation around  $I_3$  only

Rotation around  $I_2$  only: the Dzhanibekov effect

In the vicinity rather than exactly at the steady points.

A closer look

At the steady points "exactly"

Final notes on the Dzhanibekov effect

# Heavy Top

Equations in the software

Heavy top as a pendulum with spin

Pure pendulum

Effect of the spin

The three cases

Uniform motion

Simulations of the uniform motion

Discussion

The sleeping top

Discussion

# References

# Appendix

The Taylor Center software basics

Methods of loading and playing scripts

The optimal conditions for stereo viewing

# Preface

This is an Exploratorium of the rigid body motion, i.e. a collection of simulations for running via the advanced ODE solver called the Taylor Center [1], which integrates and displays real-time animation of the rigid body in 3D stereo to view through a pair of red/blue glasses, or conventionally as a 3D axonometry. For every simulation the "real-time animation" is "real-time" in the sense that the motion is displayed obeying the appropriate acceleration or deceleration within the user specified (or pre-loaded) *Play time* interval (in seconds). At that, the internal time  $t$  (analogous to the physical time) for every animation is displayed below the play time so that users can calculate the rate between the physical<sup>1</sup> and play time<sup>2</sup>.

Visualization of the rigid body here is achieved via appropriate sets of points fixed in the body. Those points outline the body as it rotates in a real-time. Such an outlining via the fixed points appears to be a reasonable compromise for the challenge of artful visualizing a rigid body in a real-time, because rendering the body surface with texture and features would be prohibitive for a real-time algorithm of the visualization.

These simulations of the rigid body motion are based upon the mathematical models presented by Dmitry Garanin [2], Mark Ashbaugh (and coauthors) [7], and Chloe Elliott [9], dynamically visualizing those models with a possibility to change the parameters and view the effects.

The three important cases of the rigid body motion considered here are:

- A rolling disk [2];
- A free top [2-7];
- A heavy top under gravity [9].

In particular here we are to consider a remarkable case of the free top spinning around the middle principle axis, mathematically analyzed in 1991, [7], and

---

<sup>1</sup>Even speaking about the physical time, in all animations here we use the internal unitless values of time, mass, length, and accelerations selected just in order that it be easier to demonstrate and play the processes of interest. For example, in the cases of *rolling disk* and *heavy top*, where gravity matters, in some cases the expression  $Mg$  is set to 1, in others - to 10. Similarly, other initial values such as angular velocities  $\omega$ ,  $\psi$  which together with  $Mg$  affect the duration and speed of the process, are chosen also merely to provide a comfortable playing time and visually detectable rotation. Therefore, when the user wishes to compare similar processes in terms of their visible speed and duration, it is necessary to check if the values  $Mg$ ,  $\omega$ ,  $\psi$  in the section Constants are the same for the processes being compared, as well as the desired internal time segment and the rate for the play time.

<sup>2</sup>The rate between the physical vs. play time is not the same in all the simulations. The pre-loaded play time in most of the simulations was chosen merely in order to be not too long and too annoying (something within 60 sec.), while the problem physical time may vary dramatically. Sometimes for sequences of simulations representing a particular case, all the crucial parameters affecting the physical time were set the same, and the play time was set in the same rate to the physical time so that the viewer could adequately perceive the "reality" of the animation. For other animations no care was taken to keep the same rate between the physical time and play time.

experimentally observed in weightlessness in 1985 by the cosmonaut Vladimir Dzhanibekov (USSR), see the video [6].

Each of the three cases requires a particular set of ODEs. Beside the ODEs in the mathematical form (as in the sources), we will show how they are entered into the software.

Below is the table of correspondence between the mathematical notation and its computer equivalents.

$\ddot{\theta}$	te1	$\zeta_x$	ksix
$\dot{\theta}$	te1'	$\zeta_y$	ksiy
$\dot{\phi}$	fi1	$\zeta_z$	ksiz
$\ddot{\phi}$	fi1'	$F_x$	Fx
$\psi$	psi	$F_y$	Fy
$\dot{\psi}$	psi1	$\pi$	Pi
$x_c$	xc	$\theta _{t=0}$	te0
$y_c$	yc	$\dot{\theta} _{t=0}$	te10
$z_c$	zc	$\dot{\phi} _{t=0}$	fi0
$I'_1$	i11	$\ddot{\phi} _{t=0}$	fi10
$I_2$	i2	$L_3$	L3
$I'_3$	i31	$L_3 _{t=0}$	L30

In this software, the systems of ODEs must be represented as systems of explicit first order ODEs, so that second order derivatives like  $\ddot{\theta}$  or  $\ddot{\phi}$  are represented via additional variables  $\dot{\theta} = \theta_1$  so that  $\ddot{\theta} = \dot{\theta}_1$  entered as

$$\begin{aligned} te' &= te1, \\ te1' &= \text{expression for this second order derivative} \\ &\dots \end{aligned}$$

Here first order derivatives in the left hand sides of the computer input are designated with apostrophe ' (ASCII code  $27_{16} = 39_{10}$ ) playing the role as the prime sign. We preserve the original notation of the referred authors, where derivatives are dotted, and prime sign in some constants (like  $I'_1$ ) has nothing to do with derivatives.

We use the terminology *angular momentum*  $\mathbf{L}$  and *principal moments of inertia*  $I_1, I_2, I_3$  of a rigid body.

The choices of particular points fixed in the body are such as 10 points on the circumference of the rolling disk, or 5 such points in a spinning symmetric top, or the vertices of spinning rectangles or triangles. In order to transform the points of the spinning body (fixed in the body and expressed via the Euler angles  $\theta, \phi, \psi$ ) into the lab system of coordinates, we use the rotation matrix (42) in [2]

$$A = \begin{pmatrix} \cos \phi \cos \psi - \cos \theta \sin \phi \sin \psi & -\cos \phi \sin \psi - \cos \theta \sin \phi \cos \psi & \sin \theta \sin \phi \\ \sin \phi \cos \psi + \cos \theta \cos \phi \sin \psi & -\sin \phi \sin \psi + \cos \theta \cos \phi \cos \psi & -\sin \theta \cos \phi \\ \sin \theta \sin \psi & \sin \theta \cos \psi & \cos \theta \end{pmatrix}$$

written for a special case when  $\psi = 0$  ( $\sin \psi = 0$ ,  $\cos \psi = 1$ ) :

$$A_0 = \begin{pmatrix} \cos \phi & -\cos \theta \sin \phi & \sin \theta \sin \phi \\ \sin \phi & \cos \theta \cos \phi & -\sin \theta \cos \phi \\ 0 & \sin \theta & \cos \theta \end{pmatrix}. \quad (1)$$

## Terminology

Here we are to clarify the terminology related to the Euler's angles (or their derivatives) often called "spin"  $\dot{\psi}$ , "precession"  $\dot{\phi}$ , and "nutation"  $\dot{\theta}$ .

Consider a vector  $\mathbf{v}(t) = (x(t), y(t), z(t))$  in resting system of coordinates. Vectors have their length  $|\mathbf{v}| = v = \sqrt{x^2 + y^2 + z^2}$  and the direction defined by the cosines  $(x/v, y/v, z/v)$ .

In particular, the speed of instantaneous rotation of a rigid body is a vector  $\boldsymbol{\omega}$ , and the absolute speed or the spin of rotation is  $|\boldsymbol{\omega}|$ . If the direction of  $\boldsymbol{\omega}$  is changing with time, we say that the spinning axis of the body performs a precession. For example, Earth spins about its axis 1 turn a day, and the axis of Earth makes a slow precession outlining approximately a surface of a right cone with a period about 26,000 years. More accurately, the axis outlines a wavy surface in which the waves are called nutation. That's the meaning in which we further understand the terms "spin", "precession", and "nutation".

Unlike Earth, an arbitrary rigid body may rotate about the center of mass in a quite irregular manner so that it is impossible to clearly distinguish its spin, precession, and nutation.

The Euler's angles are one of various ways to represent an arbitrary angular increment of vector  $\boldsymbol{\omega}$  as a sum of three consequential turns: namely by those special Euler's angles  $\theta$ ,  $\phi$ ,  $\psi$  whose velocities traditionally are also called "spin"  $\dot{\psi}$ , "precession"  $\dot{\phi}$ , and "nutation"  $\dot{\theta}$  (not a velocity). However, such naming is in conflict with the earlier defined concepts of spin, precession, and nutation, because according to the formula (15) in [2])

$$\begin{aligned} \boldsymbol{\omega} &= \dot{\theta} \mathbf{e}_N + \dot{\phi} \mathbf{e}_z + \dot{\psi} \mathbf{e}^{(3)} \\ |\boldsymbol{\omega}|^2 &= \dot{\psi}^2 + \dot{\theta}^2 + \dot{\phi}^2 + 2\dot{\psi}\dot{\phi} \cos \theta, \end{aligned}$$

so that the speed of instantaneous rotation  $\boldsymbol{\omega}$  of a body is a combination of all three Euler's angular velocities.

Similarly, speaking about the direction of  $\boldsymbol{\omega}$  in a fixed system (according to formula (18) in [2]),

$$\boldsymbol{\omega} = (\dot{\psi} \sin \theta \sin \phi + \dot{\theta} \cos \phi) \mathbf{e}_x + (-\dot{\psi} \sin \theta \cos \phi + \dot{\theta} \sin \phi) \mathbf{e}_y + (\dot{\psi} \cos \theta + \dot{\phi}) \mathbf{e}_z,$$

so that again each component of the direction of  $\boldsymbol{\omega}$  is a function of all three Euler's angles and velocities.

The terms "spin", "precession", and "nutation" applied to the Euler angles, even though holding some geometrical sense, create confusion with the meaning of these terms for a rigid body. Therefore, in order to avoid this confusion, further on we refer to the Euler's angles  $\theta$ ,  $\phi$ ,  $\psi$  just by their Greek letters.

## Installation and running the simulations

In order to run and play with these simulations, you need to download and install the software, and then the folder with the Rigid Body script files following a simple procedure explained in Appendix 1. Most of the simulations are in 3D stereo appearing as red and blue curves on the black background. You will need a pair of red/blue glasses for stereo viewing (or otherwise to view in a mode of conventional axonometry by clicking the respective button). Some simulations display conventional 2D curves (colored in different colors) appearing on the white background (for which you obviously do not need red/blue glasses).

While studying and playing with this Exploratorium, it is convenient to keep the software *Tcenter.exe* loaded. When you need to run a particular script file mentioned in this text, select and copy the file name into the clipboard and follow one of several methods of running the selected script file explained in the Appendix.



# Rolling disk

Folder: *RollingDisk*.

## The ODEs in the mathematical form

The ODEs (156), (159) in [2] for a rolling disk are:

$$\begin{aligned}\ddot{\theta} &= \frac{\left(-L_3 + I_2\dot{\phi}\cos\theta\right)\dot{\phi}\sin\theta - MgR\cos\theta + F_xR\sin\theta\sin\phi}{I_1'} \\ \frac{d}{dt}\left(\dot{\phi}\sin\theta\right) &= \frac{\left(L_3 - I_1'\dot{\phi}\cos\theta\right)\dot{\theta}}{I_2} \\ \dot{L}_3 &= MR^2\dot{\theta}\dot{\phi}\sin\theta - F_xR\cos\phi \\ \dot{x}_c &= R\left(\dot{\theta}\sin\theta\sin\phi - \frac{L_3\cos\phi}{I_3'}\right) \\ \dot{y}_c &= -R\left(\dot{\theta}\sin\theta\cos\phi + \frac{L_3\sin\phi}{I_3'}\right)\end{aligned}$$

where

$$\begin{aligned}I_1' &= \frac{I}{2} + MR^2, & I_2 &= \frac{I}{2}, & I_3' &= I + MR^2, \\ L_3 &= I_3'(\dot{\psi} + \dot{\phi}\cos\theta)\end{aligned}$$

with understanding that for a homogeneous disk  $I_1 = I_2 = \frac{I}{2}$ ,  $I_3 = I$ .

We re-wrote them using the expression for  $L_3$  into a system containing all Euler angles  $\theta$ ,  $\phi$ ,  $\psi$ :

$$\begin{aligned}\ddot{\theta} &= \frac{\left(-L_3 + I_2\dot{\phi}\cos\theta\right)\dot{\phi}\sin\theta - MgR\cos\theta + F_xR\sin\theta\sin\phi}{I_1'} & (2) \\ \ddot{\phi} &= \frac{L_3 - (I_1' + I_2)\dot{\phi}\cos\theta}{I_2\sin\theta}\dot{\theta} \\ \dot{\psi} &= \frac{L_3}{I_3'} - \dot{\phi}\cos\theta \\ \dot{L}_3 &= MR^2\dot{\theta}\dot{\phi}\sin\theta - F_xR\cos\phi \\ \dot{x}_c &= R\left(\dot{\theta}\sin\theta\sin\phi - \frac{L_3\cos\phi}{I_3'}\right) \\ \dot{y}_c &= -R\left(\dot{\theta}\sin\theta\cos\phi + \frac{L_3\sin\phi}{I_3'}\right)\end{aligned}$$

Typically the solid body motion equations are written in the rotating system of coordinates which is fixed with the rotating body. Dmitry Garanin transformed them into the laboratory system, where the disk position is expressed

via the Euler angles  $\theta$ ,  $\phi$ ,  $\psi$  (the picture on page 24 in [2]). The meaning of these angles in a case of motion of a declined disk is:

$\theta$  is the tilt of the disk to the plane ( $\dot{\theta}$  being a velocity or change of the tilt during non-uniform motion);

$\dot{\psi}$  is the angular velocity of the intrinsic rotation of the disk around its axis perpendicular to the disk at its center;

$\dot{\phi}$  is the angular velocity of the node line - the line of intersection of the disk plane and horizontal plane. In particular, if a disk is positioned perpendicularly to the plane and spins around its diameter perpendicular to the plane,  $\dot{\phi}$  is the angular velocity of this rotation.

As explained in [2],

$$L_3 = I_3'(\dot{\psi} + \dot{\phi} \cos \theta) \quad (3)$$

is a component of angular momentum.

**Remark 1** *This system of ODEs requires the initial values for  $\theta$ ,  $\dot{\theta}$ ,  $\phi$ ,  $\dot{\phi}$ ,  $\psi$ ,  $L_3$ ,  $x_c$ ,  $y_c$  at  $t = 0$ . However, considering the known equation for  $L_3$  (3),  $L_3$  and  $\psi$  are related. If we specify one, we automatically get the other. Therefore in some cases we specify  $L_3|_{t=0}$ , in others it's more convenient to specify  $\psi|_{t=0}$  instead.*

We are going to consider the following groups of cases.

1. Examples visualizing the meaning for each of the angular velocities  $\dot{\theta}$ ,  $\dot{\phi}$ ,  $\dot{\psi}$  (folder *EachAngleActions*);
2. The special cases of uniform motion when  $\theta$ ,  $\dot{\phi}$ ,  $\dot{\psi}$  remain constant (folder *UniformMotion*). The subcase when the center of the disk remains still during the motion - the so called Euler disk [5].
3. Examples of interesting dynamic from Dmitry Garanin [2] (folder *GaraninExamples*);

## Method of visualization

We achieve visualization of the moving disk via setting 11 trajectories

$$\begin{aligned} &\{x_0, y_0, z_0\} \\ &\dots \\ &\{x_9, y_9, z_9\} \\ &\{\zeta_x, \zeta_y, \zeta_z\} \end{aligned}$$

(see the page *Graph setting* in the Main window of the program). Here  $\{x_i(t), y_i(t), z_i(t)\}$  represent 10 evenly placed fixed points at the edge of the disk. For them only their motion is displayed without plotting the trace of the motion, while  $\{\zeta_x, \zeta_y, \zeta_z\}$  represents the trajectory of the Contact Point, and this trajectory is plotted. (This is achieved due to the setting *Parameters/Plot beginning with the curve # 11* in the Graph window).

## Equations in the software

Script file: *L3Declined1.scr*

### The constants.

```
Pi = 3.141592653589793238462643
p5 = Pi/5
M = 1
g=100
R = 1
MR2 = M*R^2
MgR = M*g*R
i = 1
Fx = 0
te0 = 0.5
te10 = 0
i2 = i/2
fi0 = Pi/2 {fi(0)}
i11 = i/2 + MR2 {i1'}
i31 = i + MR2 {i3'}
L30 = 10
fi10 = (L30 - sqrt( L30^2 + 4*i2*MgR * (cos(te0))^2/sin(te0))) / (2*i2*cos(te0))
```

### The Initial values

```
t = 0
te = te0
fi = fi0
Psi = 0
te1 = te10 {te'(0)}
fi1 = fi10 {fi'(0)}
L3 = L30
xc = 0
yc = 0
```

### Auxiliary variables

```
coste = cos(te)
sinte = sin(te)
cosfi = cos(fi)
sinfi = sin(fi)
cospsi = cos(psi)
sinpsi = sin(psi)
cosficoste = cosfi*coste
sinficoste = sinfi*coste
```

```

telsinte = tel*sinte
filcoste = fil*coste
zc = R*sinte {Center of mass z}
ksix = xc + R*coste*sinfi {Contact point on plane x }
ksiy = yc - R*coste*cosfi {Contact point on plane y}
ksiz = 0 {Contact point on plane z}
cospsi1 = cos(psi + p5)
sinpsi1 = sin(psi + p5)
cospsi2 = cos(psi + p5*2)
sinpsi2 = sin(psi + p5*2)
. . . . .
cospsi9 = cos(psi + p5*9)
sinpsi9 = sin(psi + p5*9)
x0 = xc + R*( cosfi*cospsi - sinficoste*sinpsi ) {a fixed point at the edge
of the disk, x}
y0 = yc + R*( sinfi*cospsi + cosficoste*sinpsi ) {a fixed edge point y}
z0 = zc + R*sinpsi*sinte {a fixed point at the edge of the disk, z}
. . . . .
x9 = xc + R*( cosfi*cospsi9 - sinficoste*sinpsi9 )
y9 = yc + R*( sinfi*cospsi9 + cosficoste*sinpsi9 )
z9 = zc + R* sinpsi9*sinte

```

Here

$$\begin{pmatrix} x_i \\ y_i \\ z_i \end{pmatrix} = A_0 \cdot \begin{pmatrix} R \cos \psi_i \\ R \sin \psi_i \\ 0 \end{pmatrix}$$

where  $A_0$  is the rotation matrix (1).

### ODEs

```

t'=1
te' = tel
fi' = fil
Psi' = L3/i31 - filcoste
tel' = ( (i2*filcoste - L3)*fi*sinte - MgR*coste + Fx*R*sinte*sinfi )/i11
fil' = (L3 - (i11 + i2)*filcoste)*tel/(i2*sinte)
L3' = MR2*telsinte*fi1 - Fx*R*cosfi
xc' = R*(telsinte*sinfi - L3*cosfi/i31) {Center of mass x}
yc' = -R*(telsinte*cosfi + L3*sinfi/i31) {Center of mass y}

```

## Visualizing the meaning for each of the angular velocities $\dot{\psi}$ , $\dot{\phi}$ , $\dot{\theta}$

(folder *EachAngleActions*)

### The meaning of $\dot{\psi}$ .

Let's begin with rotation of the disk with angular velocity  $\dot{\psi}$ . To isolate this motion, we set the tilt of the disk  $\theta|_{t=0} = \pi/2$  (perpendicularly to the plane) and  $\dot{\phi}|_{t=0} = \dot{\theta}|_{t=0} = 0$  expecting the disk roll along a straight line.

Load script file *PsiOnlySpinVert.scr* and click the *Play* button.

Watch the disk rolling with the angular velocity  $\dot{\psi} = const = 10$  (psi10=10) in vertical position with uniform speed along the straight line.

If the initial tilt of the disk  $\theta|_{t=0}$  is not perpendicular, even with initial velocities  $\dot{\phi}|_{t=0} = \dot{\theta}|_{t=0} = 0$  they will not remain zero (which we want in order to watch only  $\dot{\psi}$  effect).

We cannot set tilt  $\theta|_{t=0} = 0$  because  $\sin\theta$  is in the denominator of the equation for  $\dot{\psi}$ . We can watch however the motion when  $\theta|_{t=0}$  is near zero.

Load script file *PsiOnlySpinNearHoriz.scr* and click the *Play* button.

Watch the disk rolling near horizontally with angular velocity  $\dot{\psi}$  near 30 along a circular-like curve (though not a circle). The tilt of the disk slightly varies. In order to see that, click *Graph setting* tab in the main window. While there, click *2D* button (which clears the set of trajectories). Now specify the curve  $te(t)$ . In order to do it, first click intersection of  $t$  with X axis, and then click the intersection of  $te$  with Y axis. That would set the curve  $\{t, te\}$ . Now click *Graph*. It will show you a sine-like wave of variation of the tilt between 0.08 and 0.1 of radian.

### The meaning of $\dot{\phi}$ .

This is an angular velocity of the node line. To isolate this motion, we set the tilt  $\theta|_{t=0} = \pi/2$  (perpendicularly to the plane) and  $\dot{\psi}|_{t=0} = \dot{\theta}|_{t=0} = 0$ .

Load script file *FiOnlySpin.scr* and click the *Play* button.

Watch the disk spinning around the vertical diameter with the angular velocity  $\dot{\phi} = const = 10$  (fi10=10).

### The meaning of $\dot{\theta}$ .

This is velocity of the change of tilt  $\theta$  of the disk. To isolate this motion, we must set  $\dot{\psi}|_{t=0} = \dot{\phi}|_{t=0} = 0$ . In doing so, if we leave tilt of the disk  $\theta|_{t=0} = \pi/2$  perpendicularly to the plane, no motion may happen as this is a position of equilibrium (though unstable). In order to trigger the motion, we must either provide a small push  $\dot{\theta}|_{t=0} = 0.01$ , or set the initial tilt of the disk slightly less than  $\pi/2$ . Let's try both.

Load script file *TetaOnlyFall.scr* (with a small push  $\dot{\theta}|_{t=0} = 0.01$ ) and click the *Play* button.

The disk starts falling slowly, accelerates, and ... What?! It falls through the plane as though the plane didn't exist, continuing its motion as though a rigid pendulum.

You can see the same paradox loading script file *TetaOnlyFallPendulum.scr* (with a  $\theta|_{t=0} = \pi/2 - 0.01$ , all angular velocities being zero). Again you will see the behavior of rigid pendulum, but now swinging back and forth (and disregarding the plane too). D. Garanin refers to the similar pendulum-like behavior of the heavy top on page 19 in [2].

The explanation of this paradox is that with  $\dot{\psi} \equiv \dot{\phi} \equiv 0$  (and  $F_x = 0$ ) the first ODE of the system (2) really turns into the equation of a pendulum

$$\ddot{\theta} = -\frac{MgR \cos \theta}{I_1'} \quad (4)$$

written for an angle complementary to  $\pi/2$  so that we have cosine instead of sine (as in the standard pendulum ODE). The ODE (4) describes also the motion of a disturbed vertical stick or vertical ladder falling down presuming that such a stick-like object is fixed with a hinge as a pendulum and moves disregarding "obstacles" such as horizontal plane.

Now load script file *TetaOnlyFallWithSmallFi.scr* where we added only a negligible initial angular velocity  $\dot{\phi}|_{t=0} = 0.001$  around the vertical diameter of the disk: can such a negligible addition change the "free pendulum" behavior of the disk which falls not "noticing" the plane? Click the *Play* button.

Amazingly, now the disk does not fall and swing as a pendulum any more, but fully "acknowledges" the existence of the plane, rolling along a cycloid-like curve: almost flat falling and then standing up again, on and on!

Load *TetaOnlyFallWithSmallFiLong.scr* and watch a longer period of such motion noticing that the cycloid-like curve outlines some large circle.

Well, then how does a small  $\dot{\psi}$  affects the "fall" of a near steady disk?

Load script file *TetaOnlyFallWithSmallPsi.scr* where we added only a negligible initial angular velocity  $\dot{\psi}|_{t=0} = 0.001$  around the axis of the disk: can this negligible addition change the "free pendulum" behavior of the disk ignoring presence of the plane? Click the *Play* button.

Now the disk also does not fall through as a pendulum any more. Again it "acknowledges" the existence of the plane, but rolls along a sine-like curve: almost flat falling and then standing up again, on and on!

Load *TetaOnlyFallWithSmallPsiLong.scr* and watch a longer period of such motion noticing that now this sine-like curve outlines a straight line (rather than circle).

**Remark 2** *If the disk in the initial position slightly deviating from the vertical has zero angular velocities  $\dot{\psi}$  and  $\dot{\phi}$  so that its interaction with the plane takes place only via one point of touch at the initial position, the only force affecting the disk is gravity causing it to "fall" as a rigid pendulum ignoring existence of the plane. However, with at least one of the velocities  $\dot{\psi}$  or  $\dot{\phi}$  being nonzero,*

*the center of mass of the slightly declined disk begins moving along a curve with nonzero curvature. As a result, in addition to gravity, two more forces emerge: the centrifugal force caused by the motion along a curve, and the gyroscopic reaction caused by the gravity and precession of the axis of spin. It is these two additional forces which make the difference in the behavior of the disk in comparison with the pendulum-like behavior. More about that - in the subsection "Discussion".*

One more observation of a technical nature.

**Remark 3** *In the case TetaOnlyFall.scr of "fall", the tilt  $\theta$ , beginning with  $\pi/2$ , goes down bypassing the zero value. However, the 2nd of the ODEs (2) contains  $\sin\theta$  in the denominator. In most cases an attempt to integrate bypassing a point of singularity of the ODE fails no matter whether the solution is regular or not at this point - and with the initial values of this case the solution is regular when  $\theta = 0$ . It is because of the regularity of the solution and small values of its Taylor coefficients the program applies such a large integration step, that by mere chance it bypasses the point where  $\theta = 0$  so that the integration succeeds.*

## The special cases of uniform motion when $\theta$ , $\dot{\phi}$ , $\dot{\psi}$ remain constant

(subfolder *UniformMotion*)

Intuitively we can imagine such a physical setting that the disk rolls along the circumference with constant tilt  $0 < \theta < \pi/2$  and constant angular velocities  $\dot{\phi}$ ,  $\dot{\psi}$  in such a way that all forces acting on the disk are mutually cancelled so that the disk performs uniform motion. We are to demonstrate, that such a solution of the system (2) does exist. We assume, indeed, that  $F_x = 0$  (no external horizontal forces).

Observe that if  $\theta(t) = \text{const}$  ( $\dot{\theta} = 0$ ) is the solution of the system (2), then also  $\dot{\phi} = \text{const}$  ( $\ddot{\phi} = 0$ ),  $\dot{\psi} = \text{const}$ ,  $L_3 = I_3'(\dot{\psi} + \dot{\phi} \cos \theta) = \text{const}$  satisfy the system (2) too. With that in mind, set a condition that the right hand side of the ODE for  $\dot{\theta}$  be zero:

$$\left(-L_3 + I_2 \dot{\phi} \cos \theta\right) \dot{\phi} \sin \theta - MgR \cos \theta = 0.$$

We are to show, that it is possible to satisfy this condition for an arbitrary  $\theta$  and a few other arbitrarily given parameters. There are two approaches for solving this equation in  $\dot{\phi}$  for a given tilt  $\theta$ .

1. In addition to the given  $\theta$ , choose some value  $L_3 > 0$ . Then the equation above turns into the following square equation in  $\dot{\phi}$ :

$$I_2 \dot{\phi}^2 \cos \theta \sin \theta - L_3 \dot{\phi} \sin \theta - MgR \cos \theta = 0$$

whose solutions are

$$\dot{\phi}_{1,2} = \frac{L_3 \sin \theta \pm \sqrt{L_3^2 \sin^2 \theta + 4I_2 MgR \cos^2 \theta \sin \theta}}{2I_2 \cos \theta \sin \theta}$$

or

$$\dot{\phi}_{1,2} = \frac{L_3 \pm \sqrt{L_3^2 + 4I_2 MgR \cos^2 \theta / \sin \theta}}{2I_2 \cos \theta}. \quad (5)$$

Observe that both solutions are real. As  $\frac{4I_2 MgR \cos^2 \theta}{\sin \theta} > 0$ ,  $\dot{\phi}_{1,2}$  have opposite signs. Therefore, given constants  $\theta$  and  $L_3$ , two values of  $\dot{\phi}$  are computed based on (5), and then - the respective two values of  $\dot{\psi}$  based on (3): these two sets of values provide two uniform solutions of the source system of (2) for the given  $\theta$  and  $L_3$ .

2. In addition to the given  $\theta$ , choose some value  $\dot{\psi}$ . Then the equation above turns into the following square equation in  $\dot{\phi}$

$$\dot{\phi}^2 (I_2 - I_3') \cos \theta \sin \theta - \dot{\phi} I_3' \dot{\psi} \sin \theta - MgR \cos \theta = 0$$

whose solutions are

$$\begin{aligned}\dot{\phi}_{1,2} &= \frac{I'_3 \dot{\psi} \sin \theta \pm \sqrt{(I'_3 \dot{\psi} \sin \theta)^2 + 4MgR \cos^2 \theta (I_2 - I'_3) \sin \theta}}{2(I_2 - I'_3) \cos \theta \sin \theta} \quad (6) \\ &= \frac{I'_3 \dot{\psi} \pm \sqrt{(I'_3 \dot{\psi})^2 - 4MgR \cos^2 \theta (I'_3 - I_2) / \sin \theta}}{2(I_2 - I'_3) \cos \theta}.\end{aligned}$$

Here  $I'_3 - I_2 = I + MR^2 - \frac{I}{2} = \frac{I}{2} + MR^2 > 0$ . In order that the roots be real, it must be that

$$\dot{\psi} > \sqrt{\frac{4MgR \cos^2 \theta (I'_3 - I_2)}{I'_3 \sin \theta}} = \dot{\psi}_{thresh}$$

and then both  $\dot{\phi}_{1,2}$  are of the same sign. Therefore, given some constant  $\theta$  and  $\dot{\psi}$ , two values of  $\dot{\phi}$  are computed based on (6), and then - the respective two values of  $L_3$  based on (3): these two set of values also provide uniform solutions of the source system (2). However, unlike in the Case 1, here the initial value  $\psi$  must be big enough in accordance with the inequality above.

Let's determine the trajectory of the center of mass.

**Theorem 1** *For both of the solutions  $\dot{\phi}_{1,2}$ , the trajectory of the center of mass is a circumference with two possible radii.*

**Proof.** Assume that  $x_c$  and  $y_c$  represent some circumference with radius  $r$

$$\begin{aligned}x_c &= a - r \sin \phi \\ y_c &= b + r \cos \phi\end{aligned}$$

so that

$$\begin{aligned}\dot{x}_c &= -r \dot{\phi} \cos \phi \\ \dot{y}_c &= -r \dot{\phi} \sin \phi\end{aligned} \quad (7)$$

(in our case  $\dot{\phi} = const$ ). Re-write the equations for  $\dot{x}_c$  and  $\dot{y}_c$  in the source ODEs (2) under a condition that  $\dot{\theta} \equiv 0$

$$\begin{aligned}\dot{x}_c &= -R \frac{L_3 \cos \phi}{I'_3} \\ \dot{y}_c &= -R \frac{L_3 \sin \phi}{I'_3}.\end{aligned}$$

Comparing it with (7) we get

$$\begin{aligned}\dot{x}_c &= -r \dot{\phi} \cos \phi = -R \frac{L_3 \cos \phi}{I'_3} \\ \dot{y}_c &= -r \dot{\phi} \sin \phi = -R \frac{L_3 \sin \phi}{I'_3}\end{aligned}$$

so that the radii of the circular trajectories for two values of  $\dot{\phi}_{1,2}$  are

$$r_{1,2} = \begin{cases} R \left| \frac{L_3}{I'_3 \dot{\phi}_{1,2}} \right| & (L_3 \text{ is given}) \\ R \left| \frac{\dot{\psi}}{\dot{\phi}_{1,2}} + \cos \theta \right| & (\dot{\psi} \text{ is given}) \end{cases} \quad (8)$$

and the centrifugal acceleration<sup>3</sup> is

$$\dot{\phi}^2 r = \begin{cases} R \left| \frac{L_3 \dot{\phi}_{1,2}}{I'_3} \right| & (L_3 \text{ is given}) \\ R \left| \dot{\psi} \dot{\phi}_{1,2} + \dot{\phi}_{1,2}^2 \cos \theta \right| & (\dot{\psi} \text{ is given}) \end{cases} .$$

■

**Remark 4** For the bigger of the two  $\dot{\phi}_{1,2}$  the  $r_{1,2}$  is smaller.

**Remark 5** For the bigger of the two  $\dot{\phi}_{1,2}$  the centrifugal acceleration or the centrifugal force is bigger. In particular, if  $\dot{\phi}_2 > \dot{\phi}_1$  then

$$\text{Centrifugal}|_{\dot{\phi}_2} > \text{Centrifugal}|_{\dot{\phi}_1}, \quad (9)$$

and for the  $z$ -projections for the same tilt  $\theta$

$$\text{Centrifugal}_z|_{\dot{\phi}_2} > \text{Centrifugal}_z|_{\dot{\phi}_1}$$

acting up against the gravity, so that the following balance of forces must take place:

$$(\text{Gyroscopic}_z + \text{Centrifugal}_z - \text{Gravity})|_{\dot{\phi}_1} = (\text{Gyroscopic}_z + \text{Centrifugal}_z - \text{Gravity})|_{\dot{\phi}_2} = 0$$

or

$$(\text{Gyroscopic}_z + \text{Centrifugal}_z)|_{\dot{\phi}_1} = (\text{Gyroscopic}_z + \text{Centrifugal}_z)|_{\dot{\phi}_2}$$

so that

$$\text{Gyroscopic}_z|_{\dot{\phi}_2} < \text{Gyroscopic}_z|_{\dot{\phi}_1}. \quad (10)$$

Further on, in the examples illustrating this uniform motion, we arbitrarily choose  $\theta$  and an angular momentum  $L_3$  obtaining the rest of the initial values by the known formulas. In the following simulations we are to experiment with

---

<sup>3</sup>Two reaction forces whose sum prevents the disk from falling are the centrifugal and gyroscopic reaction: both caused by precession  $\dot{\phi}$  of the disk.

both choices of sign in the formula (5). Here are definitions of the constants for this set of problems.

```

Pi = 3.141592653589793238462643
p5 = Pi/5
M = 1
g=100
R = 1
MR2 = M*R^2
MgR = M*g*R
i = 1
Fx = 0
te0 = 0.5
te10 = 0
i2 = i/2
fi0 = Pi/2 {fi(0)}
i11 = i/2 + MR2 {i1'}
i31 = i + MR2 {i3'}
L30 = 10
fi10 = (L30 + sqrt( L30^2 + 4*i2*MgR * (cos(te0))^2/sin(te0))) / (2*i2*cos(te0))

```

The last line corresponds to formula (5), and the first "+" in it corresponds to selection of "+".

Load and play script files *L3DeclinedPlus.scr*, and then *L3DeclinedMinus.scr* paying attention to difference in the diameter of the trajectory of the center of the disk and velocity of rolling. These two cases represent the same initial value of tilt  $\theta = 0.5$  radian ( $28.6^\circ$ ). With selection of "+" in (5),  $\dot{\phi}|_{t=0} = 34.7831$ , while with selection of "-",  $\dot{\phi}|_{t=0} = -11.9933$ . In both cases the internal time segment is  $\approx 0.8$  and the playing time 8 sec. so that visually observed velocity of rolling in both cases is consistent. Given both values of  $\dot{\phi}|_{t=0}$ , we see that the absolute angular velocity of the rolling along its circle in the case "+" is about 3 times faster. You can see all these values inspecting the Debugging page.

Now load and play script files *L3NearVertPlus.scr*, *L3NearVertMinus.scr* also paying attention to difference in radii of the trajectory and velocity of rolling. These two cases represent the same initial value of tilt  $\theta = 1.4$  radian ( $80.2^\circ$ ).

With selection of "+" in (5),  $\dot{\phi}|_{t=0} = 119.37$ , internal time segment is  $\approx 0.3$ , and playing time 6 sec.

With selection of "-",  $\dot{\phi}|_{t=0} = -1.7$ , internal time segment is  $\approx 6$ , and playing time 30 sec. - i.e. 4 times shorter then it is required to preserve consistency with the case "+". You can set the playing time 120 sec. to achieve consistency and realize how slow is the motion in this "-" case.

Given both values of  $\dot{\phi}|_{t=0}$ , we see that the absolute angular velocity of the rolling along its circle in the case "+" is about 70 times faster.

$L_3 = 10, \theta = 28.6^\circ$	"+"	"-"	$L_3 = 10, \theta = 80.2^\circ$	"+"	"-"
$\dot{\phi} _{t=0}$	34.78	-11.99	$\dot{\phi} _{t=0}$	119.37	-1.7
$\dot{\psi} _{t=0}$	-25.52	15.52	$\dot{\psi} _{t=0}$	-15.28	5.28
Diameter	0.29	0.8	Diameter	0.08	5.8
Centrifugal	173.9	60	Centrifugal	596.8	8.5

The *L3NearVertPlus.scr* case behaves similarly to the exactly vertical case *FiOnlySpin.scr* ( in *RollingDisk\EachAngleAction*) considered in the section Visualizing the meaning for each of the angular velocities.

In the subfolder *PsiFixed* there are the similar script files with the same names where the given value is  $\dot{\psi}|_{t=0}$  (rather than  $L_3$ ), and then  $\dot{\phi}|_{t=0}$  and  $L_3$  obtained. The last two lines of constants there are

```

Psi10=25
fi10 = (i31*Psi10 - sqrt( (i31*Psi10)^2 + 4*(i2 - i31)*MgR * (cos(te0))^2/sin(te0)))
/ (2*(i2 - i31)*cos(te0))
L30 = i31*(Psi10 + fi10*cos(te0))

```

With all other constants as they are...

- for  $\theta = 0.1$  (files *Declined01Plus.scr* and *Declined01Minus.scr*) there must be  $\dot{\psi} > 17.24$ , ( $\dot{\psi} = 20$ );
- for  $\theta = 0.5$  (files *DeclinedPlus.scr* and *DeclinedMinus.scr*) there must be  $\dot{\psi} > 6.94$ , ( $\dot{\psi} = 8$ );
- for  $\theta = 1.4$  (files *NearVertPlus.scr* and *NearVertMinus.scr*) there must be  $\dot{\psi} > 0.94$ , ( $\dot{\psi} = 2$ ).

## The Euler Disk.

An interesting sub-case of this uniform motion is the case when the center of the mass remains still during the disk motion. Examining the ODEs (2) for  $\dot{x}_c, \dot{y}_c$ , we see that because  $\dot{\theta} = 0$ , they may be zero only if the constant  $L_3 = 0$ . That means that in order to extract the Euler case from the general case of uniform motion, we must set  $L_3 = 0$  and then getting

$$\dot{\phi} = \frac{\pm\sqrt{4I_2MgR \cos^2 \theta / \sin \theta}}{2I_2 \cos \theta} = \pm\sqrt{\frac{MgR}{I_2 \sin \theta}}.$$

That's the initial constant value for  $\dot{\phi}$  depending on the tilt  $\theta$  for the Euler case.

Load and play script files *Euler45.scr*, *EulerNear90.scr*, *EulerNearFlat.scr* displaying the uniform motion with the center of the disk resting.

## Discussion.

It's instructive to analyze all the cases of the uniform motion presented above *qualitatively*.

In the Euler case the center of mass rests, and the only force counteracting the gravity is the gyroscopic reaction. Under the gravity, the axis of rotation of the disk turns (precesses) along a direct circular cone generating a gyroscopic force having a constant component upward exactly countering the gravity.

In the general situation of the uniform rotation, the center of the mass moves along a circumference generating also a centrifugal force whose component counteracts the gravity acting upward together with the gyroscopic reaction - see the formulas (9), (10).

## Examples from Dmitry Garanin in [2]

(folder *GaraninExamples*)

The following explanation of the examples comes from the section 4.1.3 in [2].

**Example 1.** The parameters of the wheel are set to  $M = R = I = 1$ . The results show that a rolling wheel never falls on a side in spite of the gravity torque. Rolling with the rotation around the symmetry axis is pretty stable. Applied force  $F_x$  tends to accelerate the wheel's motion in the direction of the force. If the wheel's initial rotation is very slow, it nearly falls flat but, as  $\theta$  approaches 0 or  $\pi$ , the rotation dramatically increases so that both  $\dot{\phi}$  and  $\dot{\psi}$  become large and the sign of  $\dot{\theta}$  gets reversed. During the short nearly-fall time interval both the Center of Mass (CM) and the contact point assume large velocities and the contact point makes a bow around the CM. Then the wheel stands up again until the next fall on one of the sides.

One of the numerical solutions in the nearly falling regime is presented below.

Load and play the script file *NearFlatFall1.scr*.

The forces are  $Mg = 100$  and  $F_x = 0$ . The initial conditions were  $x_c(0) = y_c(0) = 0$ ,  $\theta(0) = \pi/2$ ,  $\phi(0) = \pi/2$  and  $\dot{\theta}(0) = 0.01$ ,  $\dot{\phi}(0) = 0$ ,  $\dot{\psi}(0) = -0.001$ . That is, in the initial state the wheel is upright, its plane is parallel to the  $y$ -axis and it begins rolling very slowly in the positive  $y$  direction because  $\dot{\psi}(0) < 0$ . However, a small push in the positive  $x$  direction,  $\dot{\theta}(0) = 0.01$ , together with the gravity torque cause the wheel to nearly fall flat. The CM begins to move to the right and almost reaches the surface. But because of the small initial rotation the derivatives  $\dot{\phi}$  and  $\dot{\psi}$  strongly increase and the wheel making a fast rotation with displacement stands up again.

In order to see the changes of the  $\theta$ ,  $\phi$ ,  $\psi$  load and play the script file *NearFlatFall1TeFiPsi.scr*. It demonstrates  $\theta(t)$  nearly falling and recovering.  $\phi$  shows that the wheel is rapidly precessing in alternating directions when the wheel nearly hits the ground, while  $\psi$  demonstrates at those moments how the wheel is rapidly rotating around its symmetry axis too.

Let us discuss now the motion of the Center of the Mass (CM) and of the Contact Point (CP).

In order to watch the vertical motion of the CM, in the main window under the tab *Graph setting* click *Clear* and specify the curve  $\{t, z_c\}$  by clicking first intersection of  $t$  and  $X$  axis, and then  $z_c$  and  $Y$  axis. Click *Graph*. Then the Graph window will display  $Z(t)$  and you may *Play* it to see the dynamic.

Then, in order to watch the horizontal motion of the CM and CP load and play the script file *NearFlatFall1CM-CP.scr* . One can see that as the wheel nearly touches the ground CP makes a half-circle around CM.

**Example 2.** This is the same as Example 1 except that now  $\dot{\phi}(0) = 0.25^4$ . It causes the CM of the wheel to make circles. Load and play the script file *NearFlatFall2.scr* .  $\dot{\phi}(0) > 0$  also makes the CP motion of a cycloid type.

Load and play the CM-CP curves only: *NearFlatFall2CM-CP.scr* .

**Example 3.** This is the same as Example 1 but adding also a horizontal force  $F_x = 0.03$  (while leaving  $\dot{\phi}(0) = 0.25$  as in Example 2). Load and play *NearFlatFall3.scr* : the external force makes the CM motion of a cycloid type. Watch it also in a plane version: *NearFlatFall3CM-CP.scr* .

**Example 4.** Reversing the sign of the force  $F_x = -0.03$  (with the same  $\dot{\phi}(0) = 0.25$ ) completely changes the character of the motion. Load and play *NearFlatFall4.scr* .

With a longer time interval, one can see the change of regime after some time - script file *NearFlatFall4Longer.scr* (page 35 in [2]).

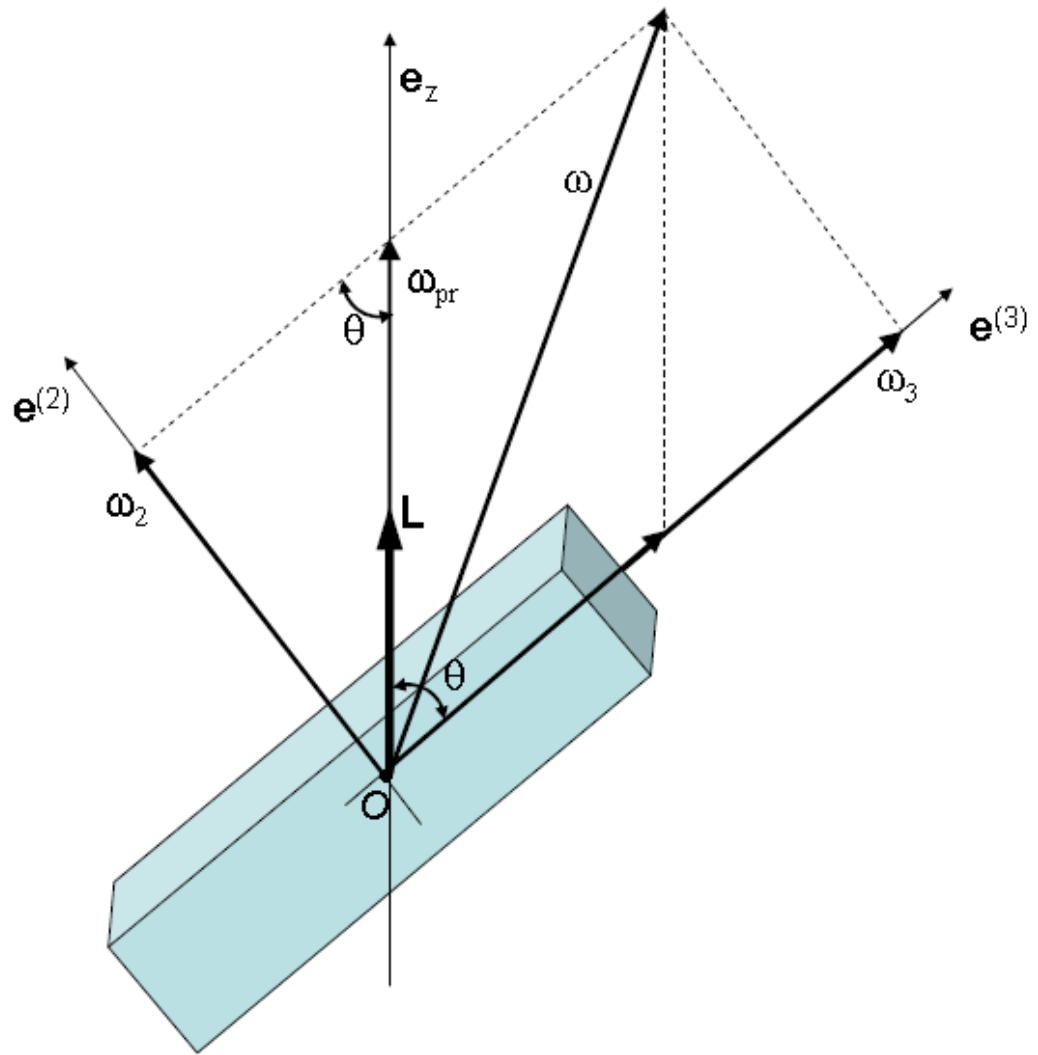
**Example 5.** With all the same but the faster  $\dot{\phi}(0) = 1$ , the motion becomes even more complicated - *NearFlatFall5.scr* .

---

<sup>4</sup>In the original article [1]  $\dot{\phi}(0) = 0.1$  and I have no clarifications from the author.

# Free top

Folder: *FreeTop*



A figure for the free top parameters from [2] p. 13

## The physical setting

Here we are considering a rigid body to which...

- a) either no forces are applied,
- b) or even if some forces are applied, their resultant force towards the rigid body is zero, and the momentum of those forces in respect to the center of the mass is zero.

The case (a) is possible only if the body is in a remote interstellar space. A more realistic setting is (b) taking place when...

1. The body freely flies in a uniform gravitational field.
2. The body freely flies in a non-uniform gravitational field being negligibly small in comparison with the variation of the field within its volume<sup>5</sup>: for example a satellite, a space probe or its part flying in the Solar system.
3. A rigid body at the surface of Earth installed in a three-ring gimbal with near zero friction at the axes so that the center of the rotating mass stays still for any position of the rings of the gimbal. The forces acting at the body in such a case are: the weight applied to the center of the mass vs. the reaction forces in the ring bearings compensating the weight in accordance with (b). If the body has an axial symmetry (say  $I_1 = I_2$ ), this arrangement represents a gyroscope (16).

## The ODEs in the mathematical form

The ODEs (86) in [2] for a free asymmetric top in original form are

$$\begin{aligned}
 \dot{\theta} &= \left( \frac{1}{I_1} - \frac{1}{I_2} \right) L \sin \theta \sin \psi \cos \psi \\
 \dot{\phi} &= \left( \frac{\sin^2 \psi}{I_1} + \frac{\cos^2 \psi}{I_2} \right) L \\
 \dot{\psi} &= \left( \frac{1}{I_3} - \frac{\sin^2 \psi}{I_1} - \frac{\cos^2 \psi}{I_2} \right) L \cos \theta = \left( \frac{L}{I_3} - \dot{\phi} \right) \cos \theta
 \end{aligned} \tag{11}$$

where  $\theta$ ,  $\psi$ ,  $\phi$  are Euler's angles. The angular momentum  $\mathbf{L} = \text{const}$  in the laboratory system,  $\mathbf{L} = \{L_x, L_y, L_z\}$  so that it is assumed  $L_x = L_y = 0$ , while  $L_z = L$ .

**Remark 6** *These ODEs demonstrate, that if the initial angular momentum  $L = 0$ , the body rests still. Otherwise, if  $L \neq 0$ , this IVP for the ODEs of a free top depend only on the initial angular positions  $\theta$ ,  $\psi$ ,  $\phi$  at  $t = 0$ .*

<sup>5</sup>Celestial bodies of a finite size in a non-uniform gravitational field do not behave as a free top because they are under various forces acting on their various parts (tidal forces).

Observe that the ODEs for  $\dot{\theta}$  and  $\dot{\psi}$  alone comprise a consistent system of two ODEs, which makes it possible later to construct a plane phase portrait  $\{\theta(t), \psi(t)\}$  for this sub-system (Fig. 1).

In the system of coordinates fixed in the body,  $I_1, I_2, I_3$  stand for the 3 principal moments of inertia of the body obeying the triangle inequalities. In order to ensure this, we arbitrarily choose three values  $a > b > c$  (in presumption that they represent the dimensions of some parallelepiped) and then we set

$$\begin{aligned} I_1 &= b^2 + c^2 \\ I_2 &= a^2 + c^2 \\ I_3 &= a^2 + b^2 \end{aligned}$$

which guarantees that values  $I_1 < I_2 < I_3$  satisfy the triangle inequalities

$$\begin{aligned} I_1 + I_2 &\geq I_3 \\ I_1 + I_3 &\geq I_2 \\ I_2 + I_3 &\geq I_1. \end{aligned}$$

For the corresponding  $L_1, L_2, L_3$  in the coordinates fixed in the body the following formulas (84) in [2] take place

$$L_1 = L \sin \theta \sin \psi, \quad L_2 = L \sin \theta \cos \psi, \quad L_3 = L \cos \theta \quad (12)$$

where  $L_1, L_2, L_3$  are components of the angular momentum in respect to the principal moments of inertia  $I_1, I_2, I_3$  fixed in the body.

Using the formulas of trigonometry

$$\sin \psi \cos \psi = \frac{1}{2} \sin 2\psi, \quad \sin^2 \psi = \frac{1 - \cos 2\psi}{2}, \quad \cos^2 \psi = \frac{1 + \cos 2\psi}{2}$$

we obtain a simpler form of the equations (11):

$$\begin{aligned} \dot{\theta} &= \frac{L}{2} \left( \frac{1}{I_1} - \frac{1}{I_2} \right) \sin \theta \sin 2\psi \\ \dot{\phi} &= \frac{L}{2} \left( \frac{1}{I_1} + \frac{1}{I_2} - \left( \frac{1}{I_1} - \frac{1}{I_2} \right) \cos 2\psi \right) \\ \dot{\psi} &= \left( \frac{L}{I_3} - \dot{\phi} \right) \cos \theta. \end{aligned} \quad (13)$$

In accordance with the formula (12), the initial values  $\theta|_{t=0}$  and  $\psi|_{t=0}$  control redistribution of the value  $L$  among the components  $L_1, L_2, L_3$  at  $t = 0$ . In particular we are interested in the following special cases.

**The special cases and the  $\{\theta(t), \psi(t)\}$  phase portrait (Fig. 1):**

1. Rotation about the axis  $I_1$  only (12):  $L_1|_{t=0} = L$  while  $L_2|_{t=0} = L_3|_{t=0} = 0$ , corresponding to the point  $\theta|_{t=0} = \pi/2, \psi|_{t=0} = \pi/2$  - a stable steady

point (Fig 1). Here  $\cos \theta = 0$ ,  $\sin \theta = 1$ ,  $\cos \psi = 0$  not only at  $t = 0$ , but the functions

$$\begin{aligned}\theta(t) &\equiv \pi/2, \quad \dot{\theta}(t) \equiv 0, \quad \cos(\theta) \equiv 0, \quad \sin(\theta) \equiv 1, \\ \psi(t) &\equiv \pi/2, \quad \dot{\psi}(t) \equiv 0, \\ \phi(t) &= \text{linear function (so that } \dot{\phi}(t) \equiv \text{const})\end{aligned}\tag{14}$$

represent a stable steady solution of the system. The spin around axis  $I_1$  is an effect of  $\dot{\phi}$  only. In computers it's impossible to set  $(\pi/2, \pi/2)$  as the initial values *exactly* (in order to obtain this steady solution *exactly*). However, with accurate approximation of  $(\pi/2, \pi/2)$ , numerical solutions  $\{\theta(t), \psi(t)\}$  evolve along an infinitely small circular loop looking like a steady solution even despite the approximate initial values.

2. Rotation about the axis  $I_2$  only (12):  $L_2|_{t=0} = L$  while  $L_1|_{t=0} = L_3|_{t=0} = 0$  corresponding to an unstable steady point  $\theta|_{t=0} = \pi/2$ ,  $\psi|_{t=0} = 0$  (Fig 1). Here<sup>6</sup> not only  $\theta = 0$ ,  $\sin \theta = 1$ , and  $\sin \psi = 0$  at  $t = 0$ , but the functions

$$\begin{aligned}\theta(t) &\equiv \pi/2, \quad \dot{\theta}(t) \equiv 0, \quad \cos(\theta) \equiv 0, \quad \sin(\theta) \equiv 1, \\ \psi(t) &\equiv 0, \quad \dot{\psi}(t) \equiv 0, \\ \phi(t) &= \text{linear function (so that } \dot{\phi}(t) \equiv \text{const})\end{aligned}\tag{15}$$

represent a solution of the system. The spin around axis  $I_2$  is the effect of  $\dot{\phi}$  only. Again, in computers it's impossible to set  $(\pi/2, 0)$  as the initial value exactly. However, unlike the Case 1 of infinitely small closed curves in the vicinity of the points  $(\pi/2, k\pi + \pi/2)$ , here the numerical integration follows either along the infinite blue trajectories (never reaching  $\theta = \pi/2$ ), or along the closed red trajectories (never reaching  $\psi = k\pi$ ). Both types approach the points  $(\pi/2, k\pi)$ ,  $k = 0, 1, \dots$  infinitely close - see Fig 1. We will demonstrate that in neighborhoods of these unstable steady points  $(\pi/2, k\pi)$  the trajectory  $\{\theta(t), \psi(t)\}$  stays during a finite time. During this time the body spins almost uniformly as though the exact solution (15). However, after expiration of this staying time, the trajectory  $\{\theta(t), \psi(t)\}$  quickly jumps along the red or blue arcs toward the next point  $(\pi/2, k\pi)$  - Fig. 1, and it is during these jumps that the physical spin of the body abruptly flips to the opposite demonstrating the Dzhanibekov effect.

3. Rotation about the axis  $I_3$  only (12):  $L_3|_{t=0} = L$  while  $L_1|_{t=0} = L_2|_{t=0} = 0$  corresponding to  $\theta|_{t=0} = 0$ . Here  $\psi|_{t=0}$  may be any value (Fig 1). Observe, that at  $t = 0$   $\cos \theta = 1$ ,  $\sin \theta = 0$ . And observe that while  $\theta(t) \equiv 0$  is a zero solution of the system, the functions  $\phi$  and  $\psi$  vary in

---

<sup>6</sup>Like the case 1, except that here  $\psi(t) \equiv 0$ .

such a way that  $\dot{\psi} + \dot{\phi} = \text{const}$ . The physical spinning around axis  $I_3$  is uniform despite being a sum of varying functions.

The following picture of trajectories  $\{\theta(t), \psi(t)\}$  was obtained using the phase portrait builder in the Taylor Center software.

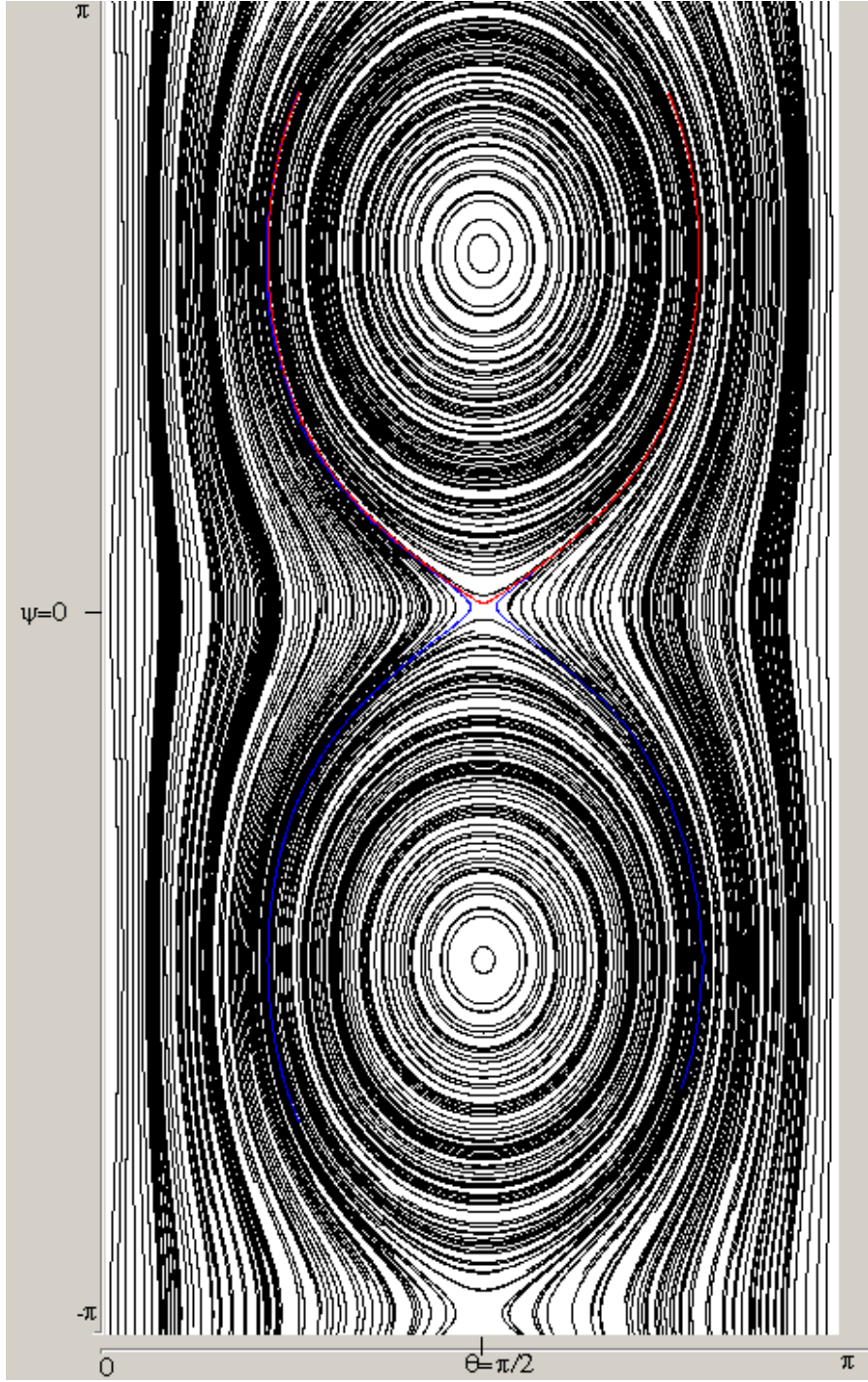


Fig. 1. Phase portrait of  $\{\theta(t), \psi(t)\} : I_1 = 6, I_2 = 11, I_3 = 15$ .

The phase portrait in Fig.1 corresponds to  $I_1, I_2, I_3$  being all different:  $I_1 < I_2 < I_3$ .

In the case of symmetry when  $I_1 = I_2$  the system (11) simplifies taking the form

$$\begin{aligned}\dot{\theta} &= 0, \quad \theta \equiv \text{const} \\ \dot{\phi} &= \frac{L}{I_1} \\ \dot{\psi} &= \left( \frac{L}{I_3} - \frac{L}{I_1} \right) \cos \theta = \text{const}\end{aligned}\tag{16}$$

As we see, in the case of  $I_1 = I_2$  the motion is uniform: angular velocities  $\dot{\phi}$  and  $\dot{\psi}$  are constant with the constant nutation angle for any initial  $\theta|_{t=0} \in [0; \pi/2]$ .

### Gyroscope.

The equations (16) representing a freely spinning body with an axis of symmetry, describe a gyroscope (case 3 in the section Physical setting earlier). When a gyroscope is being started, some rotational moment is applied to the rotor until it spins with a required velocity around the axis  $z$  so that  $L_z = L, L_x = L_y = 0, \theta = 0$ . During the starting time, the rotor is not a free top so that ODEs (16) do not apply. After the starting time ended, if the rotor was not disturbed so that  $\theta = 0$ , it is a properly functioning gyroscope whose axis holds the initial direction. Otherwise, if the rotor was disturbed during the starting time so that  $\theta \neq 0$ , after the rotor becomes a free top its axis would perform a conic precession with  $\theta \equiv \text{const} \neq 0$  so that the gyroscope would not function properly.

### The phase portrait when $I_1$ and $I_2$ are close

Contrary to the Fig 1, the  $(\theta, \psi)$  phase portrait in this case shrinks to the serious of vertical lines containing no unstable steady points. The picture below shows an approximation when  $I_1$  and  $I_2$  are close (and steady points are still present).

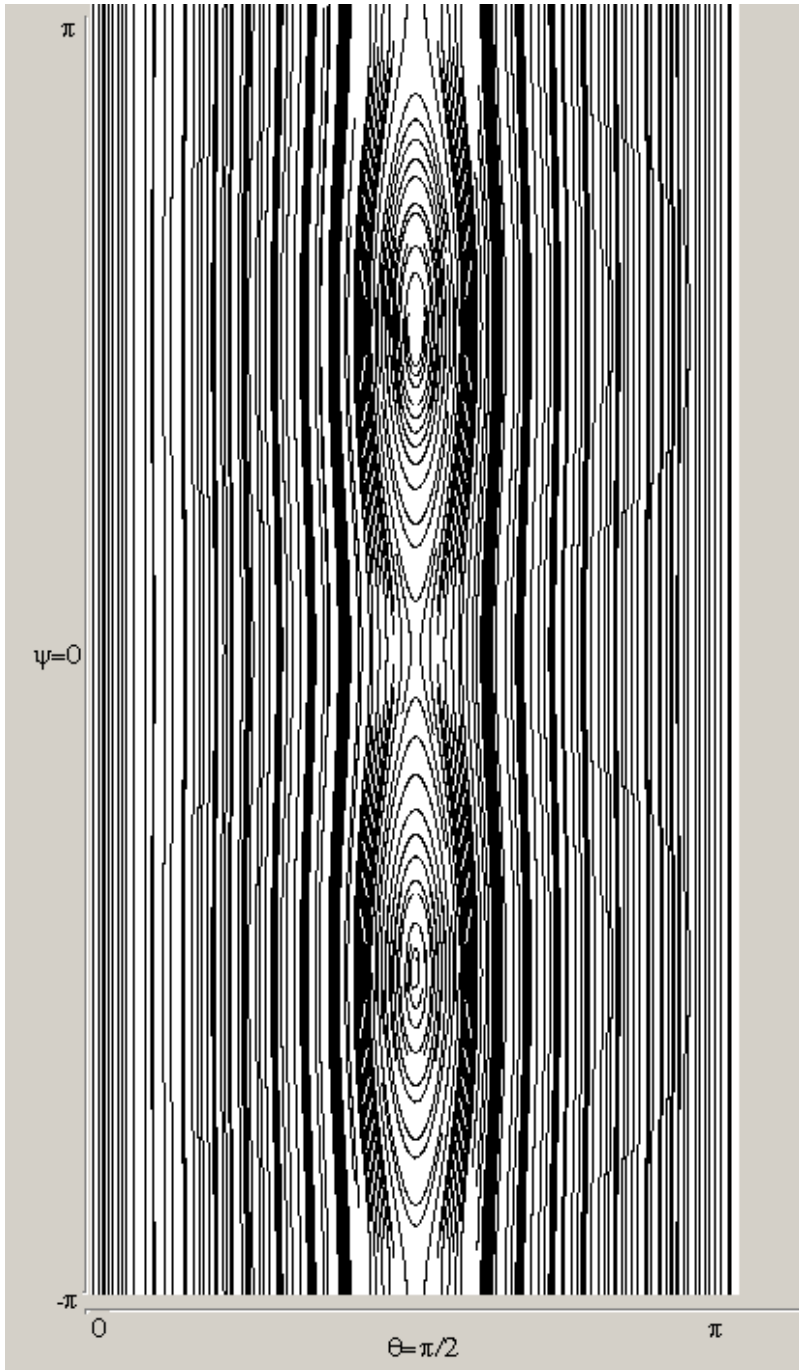


Fig. 2.  $(\theta, \psi)$  phase portrait:  $I_1 = 6$ ,  $I_2 = 6.1$ ,  $I_3 = 10.1$ .

**Remark 7** *In all of the simulations considered farther on, even when we refer to the exact cases 1-3 above, we can use only the computer approximations of the steady points (as they are expressed via irrational numbers). In other words, in all the cases of numerical simulation we operate in the "infinitely small" vicinity of the steady points excluding them.*

## Method of visualization

Here we achieve visualization of the moving body using the following simplified graphical outline. A rigid body having the principal axes  $I_1, I_2, I_3$  is represented here as a rectangle with unequal width and height. The  $\psi$  axis is perpendicular to the rectangle in its center. The rectangle is outlined with 6 points whose trajectories are entered automatically by the script file (the page *Graph setting* in the Main window of the program)

$$\begin{aligned} &\{x_1, y_1, z_1\} \\ &\dots \\ &\{x_6, y_6, z_6\} \end{aligned}$$

Here  $\{x_i(t), y_i(t), z_i(t)\}$  represent trajectories made by these points during the motion. However, the script file sets the display of the moving dots only (not plotting their trajectories).

In a few cases we also add two points on the  $\psi$  axis of the body.

For the Dzhanibekov effect the body motion is visualized also as a spinning triangle which periodically flips its orientation.

## Equations in the software

### The constants.

```
Pi = 3.141592653589793238462643
p5 = Pi/5
R = 1
H = 1.2
a2 = 4^2
b2 = 2^2
c2 = 1^1
i1 = b2 + c2
i2 = a2 + c2
i3 = a2 + b2
te0 = 0.2
fi0 = 0
Psi0 = 0.3
```

$i12 = (1/i1 - 1/i2)$   
 $i13 = 1/i3$   
 $L = 15$

### The Initial values

$t = 0$   
 $te = te0$   
 $fi = fi0$   
 $Psi = Psi0$

### Auxiliary variables

$coste = \cos(te)$   
 $sinte = \sin(te)$   
 $cosfi = \cos(fi)$   
 $sinfi = \sin(fi)$   
 $cospsi = \cos(psi)$   
 $sinpsi = \sin(psi)$   
 $fi1 = (\sinpsi^2/i1 + \cospsi^2/i2)*L$   
 $cosficoste = cosfi*coste$   
 $sinficoste = sinfi*coste$   
 $psiP10 = psi - Pi/10$   
 $cospsi0 = \cos(psiP10)$   
 $sinpsi0 = \sin(psiP10)$   
 $cospsi1 = \cos(psiP10 + p5)$   
 $sinpsi1 = \sin(psiP10 + p5)$   
 $cospsi5 = \cos(psiP10 + p5*5)$   
 $sinpsi5 = \sin(psiP10 + p5*5)$   
 $cospsi6 = \cos(psiP10 + p5*6)$   
 $sinpsi6 = \sin(psiP10 + p5*6)$   
 $x0 = R*(cosfi*cospsi0 - sinficoste*sinpsi0)$   
 $y0 = R*(sinfi*cospsi0 + cosficoste*sinpsi0)$   
 $z0 = R*sinpsi0*sinte$   
 $x1 = R*(cosfi*cospsi1 - sinficoste*sinpsi1)$   
 $y1 = R*(sinfi*cospsi1 + cosficoste*sinpsi1)$   
 $z1 = R*sinpsi1*sinte$   
 $x5 = R*(cosfi*cospsi5 - sinficoste*sinpsi5)$   
 $y5 = R*(sinfi*cospsi5 + cosficoste*sinpsi5)$   
 $z5 = R*sinpsi5*sinte$   
 $x6 = R*(cosfi*cospsi6 - sinficoste*sinpsi6)$   
 $y6 = R*(sinfi*cospsi6 + cosficoste*sinpsi6)$   
 $z6 = R*sinpsi6*sinte$   
 $x7 = 0.5*(x0 + x6)$   
 $y7 = 0.5*(y0 + y6)$   
 $z7 = 0.5*(z0 + z6)$

```

x8 = 0.5*(x1 + x5)
y8 = 0.5*(y1 + y5 )
z8 = 0.5*(z1 + z5 )
x10 = -H*sinte*sinfi
y10 = H*sinte*cosfi
z10 = -H*coste
x11 = 0
y11 = 0
z11 = 0
x12 = -x10
y12 = -y10
z12 = -z10

```

Here the points of the circumference ( $i = 0, \dots, 9$ )

$$\begin{pmatrix} x_i \\ y_i \\ z_i \end{pmatrix} = A_0 \cdot \begin{pmatrix} R \cos \psi_i \\ R \sin \psi_i \\ 0 \end{pmatrix}$$

while the point on the  $\dot{\psi}$  axis

$$\begin{pmatrix} x_{10} \\ y_{10} \\ z_{10} \end{pmatrix} = A_0 \cdot \begin{pmatrix} 0 \\ 0 \\ -H \end{pmatrix}$$

( $A_0$  is the rotation matrix (1)).

### ODEs

```

t' = 1
te' = i12*L*sinte*sinpsi*cospsi
fi' = fi1
psi' = (L/i3 - fi1)*coste

```

## General position cases

To begin with, consider a symmetric free top when  $I_1 = I_2$  ( $a_2=b_2$ ) so that the equations (11) turns into (16) ( $\theta = 0.1$  (radian),  $\psi = 0$ ). Load the script *SymPi10.scr* and click the *Play* button. Observe a uniform motion when  $I_3$ -axis outlines a right circular cone. Here the program plots a trajectory of the end point of  $I_3$  axis of the rotation  $\dot{\psi}$ . Unlike asymmetric cases later, here the motion is uniform at *any* initial tilt  $\theta|_{t=0} \in [0; \pi/2]$ .

Now consider an asymmetric case in some general position ( $\theta = 1$  (radian),  $\psi = 0$ ) loading script file *genTe1Psi0.scr* and clicking the *Play* button. Here

too the program plots a trajectory of the end point of  $I_3$  axis. Watch that tilt  $\theta$  varies along with  $\phi$ .

Then load *PlaneTe1Psi0t.scr* for the same settings. It demonstrates that not only  $\theta$  varies, but that also spinning around  $I_3$ -axis is not uniform having varying velocity. That's a typical situation for an asymmetric free top motion, when the spinning velocity around  $I_3$ -axis generally is not constant interacting with varying  $\theta$  and  $\phi$ .

## Rotation around $I_1$ only

Here we are to see a simulation of the Case 1:  $L_1 = L$  ( $L_2 = L_3 = 0$ ,  $\theta = \pi/2$ ,  $\psi = \pi/2$  at  $t = 0$ ) according to (12). The points ( $\theta = \pi/2$ ,  $\psi = \pi/2 + k\pi$ ),  $k = 0, \pm 1, \pm 2, \dots$ , are stable steady point - see the phase portrait Fig 1.

Load script file *L1only.scr* and click the *Play* button. Watch the rotation around the axis  $I_1$  of the smallest momentum (along the long axis of the rectangle). This rotation looks uniform - and is in fact uniform with the exact solution  $\theta(t) \equiv \pi/2$ ,  $\psi(t) \equiv \pi/2$ , and the rotation velocity expressed via  $\dot{\phi} = const$  only.

## Rotation around $I_3$ only

Here we are to see a simulation of the Case 3:  $L_3 = L$  ( $L_1 = L_2 = 0$ ,  $\theta = 0$  at  $t = 0$ ) according to (12) - see Fig 1.

Load script file *L3only.scr* and click the *Play* button. Watch the rotation around the axis  $I_3$  of the biggest momentum (rotation around the axis perpendicular to the rectangle). Observe that spinning around  $I_3$  is slower than around  $I_1$ . The duration of both segments (in unitless time) is about 1 played the same 10 seconds in both cases.

This rotation also looks uniform - and it is, however this fact must be established, because though  $\theta(t) \equiv 0$ , neither of the velocities  $\dot{\psi}$  or  $\dot{\phi}$  are constant. Considering that

$$\dot{\psi} = \left( \frac{L}{I_3} - \dot{\phi} \right) \cos \theta$$

and  $\cos \theta \equiv 1$ , and according to the formulas (18) in [2]

$$\begin{aligned} \omega_1 &= \dot{\phi} \sin \theta \sin \psi + \dot{\theta} \cos \psi \\ \omega_2 &= \dot{\phi} \sin \theta \cos \psi - \dot{\theta} \sin \psi \\ \omega_3 &= \dot{\phi} \cos \theta + \dot{\psi}. \end{aligned}$$

we see that  $\omega_3 = \dot{\phi} \cos \theta + \dot{\psi} = \frac{L}{I_3} = const$ , though  $\dot{\psi}$  and  $\dot{\phi}$  are not constant! Load script file *L3onlyFi1Psi1Te1.scr* and watch the violent oscillation of  $\dot{\phi}$  (compensated with just as violent oscillation of the  $\dot{\psi}$  so that  $\theta$ ,  $\omega_3$  and  $L_3$  remain constant). We clearly see here that the Euler's angular velocities  $\psi$  and  $\phi$  have little to do with the actual spin  $\omega_3$  of the body.

## Rotation around $I_2$ only: the Dzhanibekov effect

Sub-folder *L2*.

As we saw above in the initial descriptions of the three cases, also in this case 2 there exists an exact solution (15) of the uniform rotation similar to the solution (14) in the Case 1. It's easy to write down a special trivial system of ODEs (having nothing to do with the system (11)) satisfied by this special solution (15), which shows that the rotation of the body takes place due to the linear nonzero function  $\phi(t)$  only,  $\theta$  and  $\psi$  being constants.

The difference with the Case 1 however is in that neither in physical world, nor in numerical integration the exact solution of the *original system* (11) for the initial points ( $\theta = \pi/2$ ,  $\psi = k\pi$ ) is achievable because we always deal with solutions for some approximations of those steady points ( $\theta = \pi/2$ ,  $\psi = k\pi$ ). It will be demonstrated (Theorem 2 below) that in the vicinity of the steady points the rotation of the body also takes place due to the "almost" linear nonzero function  $\phi(t)$  only, while  $\theta$  and  $\psi$  are almost constants, whose constancy is periodically violated by surges - the flipping of the Dzhanibekov effect.

At the beginning, just like in the cases of the axes  $I_1$  and  $I_3$ , rotation around  $I_2$  also looks as though uniform, however it does not remain uniform infinitely long. After certain period of uniformity, the body quickly flips its orientation for the opposite in respect to  $I_2$ , continuing the flipped uniform rotation around it, then it flips again, and so on.

The theoretical instability of rotation around the middle axis  $I_2$  was known already for long since 1851 thanks to Poincot [8]. Later this effect was observed during rotation of some objects also in reality, particularly for a tennis racket, studied by Mark Ashbaugh [7] in 1991. However, it required weightlessness in order to watch the *lasting* spin of a free rigid body with three different principle axes demonstrating this effect, and so it happened to be the astronaut Dzhanibekov (1985) who first noticed this remarkable behavior of a spinning wingnut depicted in the video [6].

Watch this video of real physical objects displaying the Dzhanibekov effect, and then load the script files demonstrating mathematical simulation of this effect: first - the file *L2only.scr* (a spinning frame with a handle), and then *L2onlyAsTriang.scr* (a spinning triangle). Both objects in these simulations spin and flip like the real things in the video, which is remarkable in itself.

In all the simulations below (except one) we use the same distinct moments of inertia  $I_1 = 6$ ,  $I_2 = 11$ ,  $I_3 = 15$ . The exceptional one with near symmetrical moments  $I_1 = 6$ ,  $I_2 = 6.1$ ,  $I_3 = 10.1$  is *L2onlyAlmSym.scr*. Load and play it observing that in it the Dzhanibekov flip also takes place, but much later.

### In the vicinity rather than exactly at the steady points.

The point ( $\theta = \pi/2$ ,  $\psi = 0$ ) defining the Case 2 is an unstable steady point among infinitely many such unstable steady points ( $\theta = \pi/2$ ,  $\psi = k\pi$ ),  $k =$

0, 1, ... along the central vertical line in the phase portrait Fig 1. We are to demonstrate that it is this set of these points of instability which is responsible for the remarkable behavior in the Dzhanibekov effect. At that, no numerical solution can reproduce the exact infinitely steady solution (14). No trajectory  $\{\theta(t), \psi(t)\}$  reaches the points  $(\pi/2, k\pi)$ , though closely approaching them. During such approaches,  $\theta$  is close to  $\pi/2$ , and according to the ODEs (11),  $\dot{\theta}(t)$  and  $\cos\theta(t)$  remain close to 0. It is then that we see the lasting uniform rotation of the body in fixed orientation after which it flips.

### A closer look.

After watching in stereo a quite realistic simulation of the flipping, let's take a closer look at the details of this flipping. The most direct indicator of the flipping is the moments  $L_1(t), L_2(t), L_3(t)$  (12) showed at the Fig 3. This picture displays various versions of the curves  $L_1(t), L_2(t), L_3(t)$  for different initial values approximating the exact steady point  $(\theta = \pi/2, \psi = 0)$ . The curve named "exact" represents the best machine approximation of  $\pi$  up to 19 decimal digits.

All the curves have a plateau whose width depends on the closeness of the initial point to the exact  $(\theta = \pi/2, \psi = 0)$ . We see that all three moments have their plateau simultaneously,  $L_1 = L_3 = 0, L_2 = \pm const \neq 0$  (in red). It's during the time segments corresponding to those plateau when the body spins near uniformly. Then, in a short time of flipping,  $L_2$  (in red) flips to the opposite values, while  $L_1$  and  $L_3$  after a short surge return to their zero state.

**Remark 8** *Observe that only in the "exact" case of the initial values the surges of  $L_1$  and  $L_3$  are irregular, while in the approximate cases they are regular. Observe also that only in the "exact" case the first plateau is significantly wider than the other plateaus in the same curve. These effects take place only for the "exact" initial values, which will be explained later.*

In order to understand better the origins of those plateaus in all  $L_i(t)$ , it is instructive to watch the behavior of  $\psi(t), \theta(t)$  in comparison with  $\sin\theta(t)$  and  $\cos\psi(t)$  - as the formulas (12) for the  $L_i$  suggest.

We are to experiment now with the case when the initial values  $\psi = 0.1, \theta = \pi/2$ : slightly higher than the steady point so that the trajectory  $\{\theta(t), \psi(t)\}$  is a closed curve in the red zone in the Phase portrait Fig. 1.

Load the script file *TePsiSinteCosPsiPsi01.scr* corresponding to this case. You will see 4 curves:  $\theta(t)$  in black,  $\psi(t)$  in red,  $\sin\theta(t)$  in blue, and  $\cos\psi(t)$ . Observe that  $\theta(t)$  and  $\psi(t)$  are smoother than  $\sin\theta(t)$  and  $\cos\psi(t)$ . The  $\sin\theta(t)$  and  $\cos\psi(t)$  display sharper and wider plateaus, and the width of the plateaus determines the steady time or duration of the uniform spin.

Now load the script file *Psi(te)Psi01.scr* corresponding to the same case, but showing the trajectory  $\{\theta(t), \psi(t)\}$ . Play it and watch how the bullet slows down at the bottom and the top of the curve where the curve approaches the steady point  $(\theta = \pi/2, \psi = k\pi)$ . This slowing down turns into a significant

pause in the next case where the distance to the exact steady point is very small - load and play file *Psi(te)Psi0000001.scr*.

Now let's explore the same effects for the blue trajectories  $\{\theta(t), \psi(t)\}$  in Fig. 1 for which initial values  $\psi = 0$  exactly, but  $\theta$  slightly deviates from  $\pi/2$ . Load the script *TePsiSinteCosPsiTe15.scr* where  $\theta = 1.5$ .

Again you will see 4 curves:  $\theta(t)$  in black,  $\psi(t)$  in blue,  $\sin\theta(t)$  in magenta, and  $\cos\psi(t)$  in green. However, unlike in the previous case,  $\psi(t)$  now is a stair like curve as it should being in the blue zone of the Phase portrait Fig 1. Here too,  $\theta(t)$  and  $\psi(t)$  display smoother plateaus than those in  $\sin\theta(t)$  and  $\cos\psi(t)$ .

Now load and play *Psi(te)Te15.scr*. Unlike in the previous case, this blue-type  $\{\theta(t), \psi(t)\}$  trajectory leads from one to the next of the steady points ( $\theta = \pi/2, \psi = k\pi$ ) and so on, resting in the vicinity of each of them. This rest time becomes longer in the next sample when initial value  $\theta = \pi/2 - 0.00001$  : load and play *Psi(te)Te00001.scr* .

Now let's try the initial value with just one zero more after the decimal point so that  $\theta = \pi/2 - 0.000001$  - load *Psi(te)Te000001.scr* . To our surprise, what we expected to be the blue-type trajectory going up and down infinitely, now turned into the already familiar coconut-type closed curve in the red zone (Fig. 1). And if you play it, it pauses at the top and bottom just like the red trajectories do - despite that the initial value ( $\theta = \pi/2 - 0.000001, \psi = 0$ ) corresponds to the blue type trajectories.

We have just seen the effect of the well known [8] instability of the ODEs (11) surfaced in this integration process at the given (default) accuracy settings, at which the integration along the blue-type trajectory from the point ( $\theta = \pi/2 - 0.000001, \psi = 0$ ) slipped into the red zone near the next steady point ( $\theta = \pi/2, \psi = -\pi$ ) - as the red and blue zones are infinitely close to each other - Fig. 1.

Now let's load the sample *Psi(te)Te000001blue.scr* with the same initial values ( $\theta = \pi/2 - 0.000001, \psi = 0$ ) but more stringent integration step parameter  $k = 0.1$  (instead of the default  $k = 0.5$ ). With this higher accuracy of integration we see that trajectory  $\{\theta(t), \psi(t)\}$  got back into the blue zone, as it should.

**Conclusion 1** *When close enough to the steady points ( $\theta = \pi/2, \psi = k\pi$ ), the integration process of the system (11) is so sensitive, that slipping from the red to blue zone trajectories and vice versa (Fig. 1) may take place. The slipping happens even despite the fact that the Taylor integration method potentially promises the highest accuracy up to all digits of the mantissa in the float point numbers (63 binary digits in the PC type "extended" used in this software). However, this goal may not be always achieved because of the so called catastrophic subtraction (or cancellation) error emerging in some unstable problems like this one. It's a catastrophic loss of significant digits because of a cancellation in a difference*

of two close non-zero numbers in a fixed length float point representation. For example, an attempt to compute a derivative of a differentiable function  $f'(x)$  via a finite difference

$$f'(x) \approx \frac{f(x + \delta) - f(x)}{\delta}, \quad \delta = 2^{-n}$$

for a small enough  $\delta$  in a fixed float point format will yield zero rather than the derivative. In Automatic Differentiation we do not deal with such finite differences thanks to availability of the formulas for  $n$ -order differentiation for elementary functions. However a catastrophic cancellation may emerge in the right hand sides of ODEs and while computing their derivatives by the formulas of AD.

### At the steady points "exactly"

"Exactly" in computers means with the best possible accuracy: for the PC it's 19 accurate decimal digits of  $\pi$  (or 63 binary digits). In this section we are to consider simulations with the initial values  $(\theta = \pi/2, \psi = k\pi)$  at the steady points specified with such accuracy. In the PC any approximation of  $\pi/2$  differs<sup>7</sup> from  $\pi/2$  so that even with the exact  $\psi = 0$  these initial values in exact mathematical terms surely correspond to the blue zone trajectories. However in numerical implementation, as we saw in the examples above, even a difference  $10^{-7}$  from the exact  $\pi/2$  suffices to cause slipping of the trajectory from the blue into the red zone. Therefore...

1. With the difference as small as about  $10^{-18}$  from the exact value  $\pi/2$  in the initial values, a random drift (though negligibly small) of the trajectory  $\{\theta(t), \psi(t)\}$  between the red and blue zones takes place in a small vicinity of the steady points - until the trajectory finally gets away from the steady point far enough to further follow one of the 8 possible routes: 4 in the blue zone, or 4 in the red zone - Fig 1.
2. As we have discussed earlier, while in a vicinity of the steady points  $(\theta = \pi/2, \psi = k\pi)$ , the trajectory  $\{\theta(t), \psi(t)\}$  (when played) slows down and rests for a certain time: the closer to the steady point - the longer. Take a look at the Fig. 3 displaying all momenta  $L_i(t)$ ,  $i = 1, 2, 3$ :  $L_2(t)$  in red. The item 1 in Fig. 3 corresponds to the "exact", i.e. 19 digits accurate decimal approximation of the initial values - the closest possible. In it we see the first plateau being the largest corresponding to the longest staying time. This longest staying episode ends when the integration takes one of the possible 8 ways reaching a vicinity of the next steady point

---

<sup>7</sup>Even if we did not need  $\pi$  in our numerical model, in the float point format most of rational numbers also cannot be represented exactly, and rounding errors are inevitable. Exact integration of a solution corresponding to a particular initial value (in the float point format) is a rare exception.

$(\theta = \pi/2, \psi = k\pi)$  - though never approaching it with the accuracy as high as the initial accuracy  $10^{-18}$  at the first plateau. That is why all the subsequent plateaus are shorter.

Navigate into the subfolder *FreeTop\L2\Unpredictable*. It contains several versions of the same problem with the "exact" initial values  $(\theta = \pi/2, \psi = 0)$  integrated with different values of the integration step ratio (specified on the Integration setting page of the Main window). Let's begin with the simulation for the ratio 0.5 (appearing in the file names as 05).

Load script *k05Te(t)Psi(t).scr* displaying the functions  $\theta(t)$  and  $\psi(t)$ . Recall that both functions theoretically must be constants like the steady solution (14):  $\theta \equiv \pi/2, \psi \equiv 0$ . However  $\psi(t)$  behaves like a stair with steps randomly drifting up or down. As it was mentioned in the beginning, it is the function  $\phi(t)$  only which is responsible for rotation of the body.

Load script *k05TePsiFi(t).scr* displaying the same graphs  $\theta(t), \psi(t)$  adding  $\phi(t)$ . You see that  $\phi(t)$  near linearly grows no matter how  $\psi(t)$  drifts and which direction  $\theta(t)$  surges.

Load script *k05Psi(Te).scr* displaying the trajectory  $\{\theta(t), \psi(t)\}$  and then Play it keeping the Phase portrait Fig. 1 at hand. First the bullet pauses at  $(\theta = \pi/2, \psi = 0)$ . Then it jumps to  $(\pi/2, \pi)$  and pauses there. Then it jumps to  $(\pi/2, 2\pi)$ , pauses, and jumps back to  $(\pi/2, \pi)$  in accordance with the graph *k05Te(t)Psi(t).scr*. As this graph suggest, judging by the oscillation of  $\psi(t)$ , the last loops are along the red type trajectories. The following simulations are with the integration ratio 0.05.

*k005Te(t)Psi(t).scr* shows randomly drifting steps of a stair again (though in a different way), while...

*k005Te(t)Psi(t)Fi(t).scr* adds  $\phi(t)$  which evolves near linearly disregarding the randomness of  $\theta(t)$  and  $\psi(t)$ .

*k005Psi(te).scr* displays the trajectory  $\{\theta(t), \psi(t)\}$  which you must Play and also compare with the Phase portrait Fig. 1

**Conclusion 2** *Because of instability at the unstable steady points  $(\theta = \pi/2, \psi = k\pi)$ , the behavior of the curve  $\{\theta(t), \psi(t)\}$  in small vicinity of these points is unpredictable. At every such point there are as many as 8 possible ways how the curve  $\{\theta(t), \psi(t)\}$  may further evolve (Fig. 1). Yet despite these 8 unpredictable routes for the trajectory  $\{\theta(t), \psi(t)\}$ , the following Theorem takes place.*

**Theorem 2** *In the close vicinities of the unstable steady points  $(\theta = \pi/2, \psi = k\pi)$  the motion is steady for any of the curves  $\{\theta(t), \psi(t)\}$  so that the body spins uniformly at these points, until it jumps away along one of 8 possible ways. Whichever of the 8 ways the curve  $\{\theta(t), \psi(t)\}$  takes, when reaching any of the 2 neighboring unstable steady points  $(\theta = \pi/2, \psi = k\pi)$ , the rotation momentum  $L_2$  switches its sign to the opposite making the flip.*

**Proof.** As it follows from the ODEs (11), in the vicinity of points  $\theta = \pi/2$ ,  $\psi = k\pi$  the values  $\theta$  and  $\psi$  are near zero meaning the evolution of the curve  $\{\theta(t), \psi(t)\}$  pauses and the body uniformly spins with the velocity  $\dot{\phi}$  until it "jumps". Recalling that  $L_2 = L \sin \theta \cos \psi$ , the function  $\cos \psi$  changes the sign from +1 to -1 and vice versa at the points  $\psi = k\pi$ , while  $\sin \pi/2$  remains 1, which proves the Theorem. ■

This Theorem provides an explanation why the graph  $L_2(t)$  (red) switches the sign from +1 to -1 and vice versa *regularly*, while  $L_1(t)$ ,  $L_3(t)$ , as well as  $\theta(t)$ ,  $\psi(t)$ , and  $\dot{\phi}(t)$  may switch the signs irregularly during the flips. This regular flipping of  $L_2(t)$  is easily observable both in the video of the physical experiment of Dzhanibekov, and in numerical simulations in 3D in this software. It's more challenging to notice the irregular surges of  $\theta(t)$ ,  $\psi(t)$  in 3D simulations, but the 2D graphs display surges of  $\theta(t)$ ,  $\psi(t)$ , and  $\dot{\phi}(t)$  with the best clarity.

The samples *Psi(te)Psi01.scr*, *Psi(te)Psi0000001.scr*, *Psi(te)Te15.scr* in subsection "Closer look" well demonstrate the pausing in the vicinities of the points ( $\theta = \pi/2$ ,  $\psi = k\pi$ ).

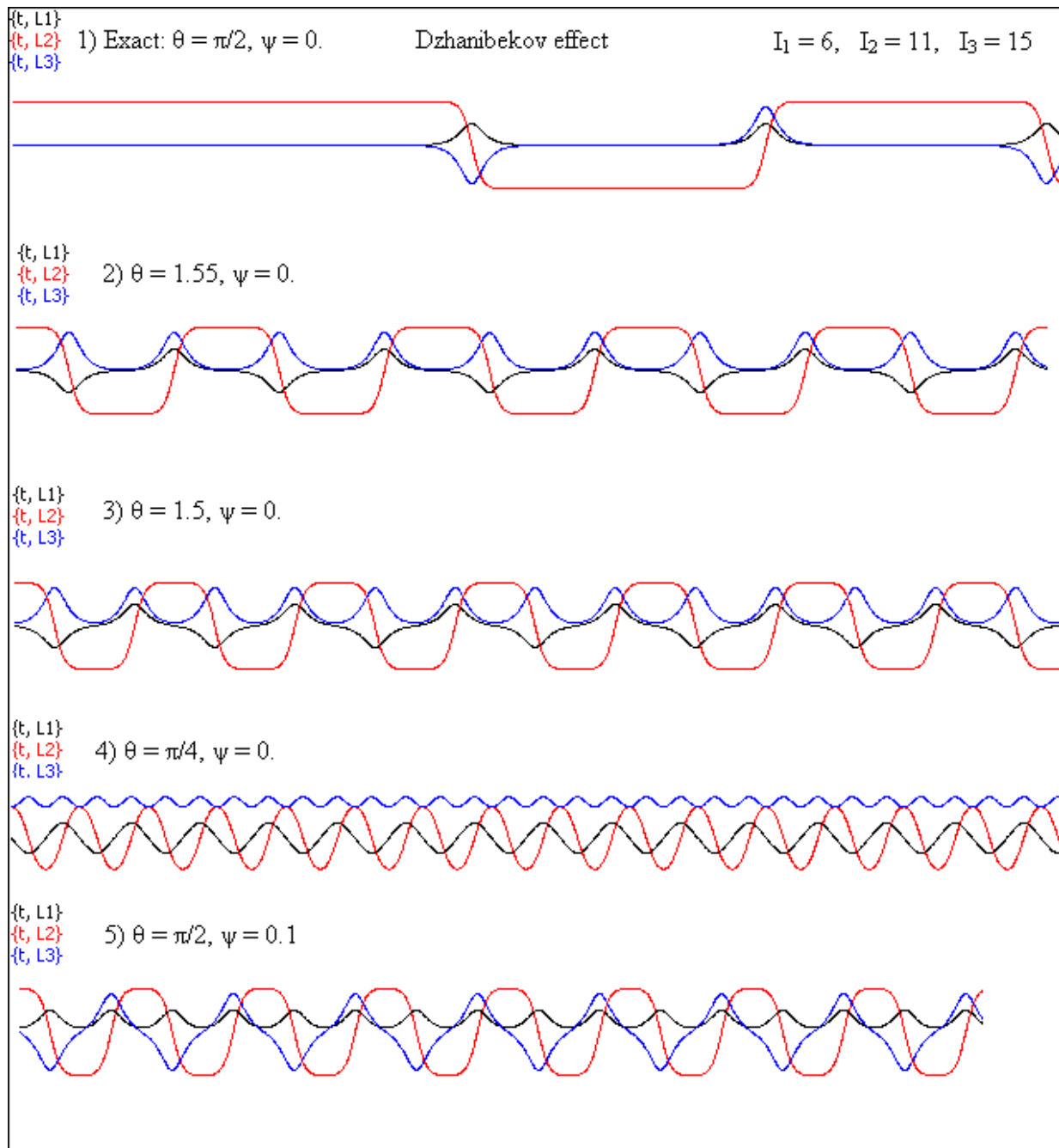


Fig. 3. Momenta  $L_i$  for various initial values in the vicinity of steady points.

## Final notes on the Dzhanibekov effect

The Dzhanibekov effect is a consequence of the remarkable behavior of the solutions of the system (11) in the vicinity of all unstable steady points ( $\theta = \pi/2$ ,  $\psi = k\pi$ ). As a result of the instability, instead of escaping into a chaotic behavior, the trajectories  $\{\theta(t), \psi(t)\}$  approaches the next point ( $\theta = \pi/2$ ,  $\psi = k\pi$ ) by one of 8 possible escape routes, pausing at every such point while the body performs approximately uniform rotation.

- In the physical world, a wingnut easily spinning on a fixed bolt in weightlessness, presents near ideal mechanical arrangement. When an astronaut strongly spins the wingnut so that it moves toward the end of the bolt, the nut leaves the bolt uniformly moving and spinning around its middle axis  $I_2$  with high enough accuracy. However, in the real world there are some physical disturbances such as turbulence in air, or small mechanical inaccuracies. Therefore, the wingnut rotation corresponds to the behavior of the mathematical model in the close vicinity of the steady points ( $\theta = \pi/2$ ,  $\psi = k\pi$ ) (rather than the special solution (15)).
- In numerical simulations the exact initial values for the special solution (15) cannot be even specified. Moreover, because of the instability of the system (11) near the unstable steady points, integration of the ODEs in the vicinity of those points even with the Taylor method adds inaccuracies acting similar to the disturbances in the physical world. That is why we can observe the Dzhanibekov effect both in physical world and in these numeric simulations.

## Heavy Top

Folder: *HeavyTop*.

Here we refer to the theory of the heavy top motion as it is presented in the article "The spinning top" by Chloe Elliott [9]. The ODEs (3.73)-(3.75) for a heavy top in the original form in [9] are

$$\begin{aligned}\dot{u}^2 &= f(u) \\ \dot{\phi} &= \frac{b-au}{1-u^2} \\ \dot{\psi} &= \frac{I_1 a}{I_3} - u \frac{b-au}{1-u^2},\end{aligned}\tag{17}$$

where

$$\begin{aligned}u &= \cos \theta \\ f(u) &= (1-u^2)(\alpha - \beta u) - (b-au)^2\end{aligned}\tag{18}$$

and the meaning of the constants are

$$\begin{aligned}
a &= \frac{I_3 \omega_3}{I_1}, \quad b = \frac{p_\phi}{I_1} = \dot{\phi} \sin^2 \theta + a \cos \theta \\
V_{eff} &= \frac{I_1 (b - a \cos \theta)^2}{2 \sin^2 \theta} + Mgl \cos \theta \\
E' &= \frac{1}{2} I_1 \dot{\theta}^2 + V_{eff} \\
\alpha &= \frac{2E'}{I_1}, \quad \beta = \frac{2Mgl}{I_1},
\end{aligned} \tag{19}$$

An alternative form for (17) is in  $\theta$  directly:

$$\dot{\theta} = \sqrt{\alpha - \beta \cos \theta - \frac{(b - a \cos \theta)^2}{\sin^2 \theta}}.$$

In both cases above, the  $\dot{u}$  and  $\dot{\theta}$  are expressed via a square roots of the right hand sides creating a difficulty for the Taylor integration when the under-root expression approaches zero (a singularity point). Therefore we rewrite these equations into a second order ridding of the square root:

$$\begin{aligned}
\ddot{u} &= \frac{3}{2} \beta u^2 - (\alpha + a^2)u - \frac{\beta}{2} + ab \\
\dot{\phi} &= \frac{b - au}{1 - u^2} \\
\dot{\psi} &= \frac{I_1 a}{I_3} - u \dot{\phi}
\end{aligned} \tag{20}$$

or

$$\begin{aligned}
\ddot{\theta} &= \frac{\beta}{2} \sin \theta + \frac{(a \cos \theta - b)(a - b \cos \theta)}{\sin^3 \theta} \\
\dot{\phi} &= \frac{b - a \cos \theta}{\sin^2 \theta} \\
\dot{\psi} &= \frac{a I_1}{I_3} - \dot{\phi} \cos \theta
\end{aligned} \tag{21}$$

both used for integration.

Similarly to the case of a "rolling disk" without rolling (considered earlier in a subsection "The meaning of  $\dot{\theta}$ "), the motion of a heavy top also relates to mathematical pendulums: here is how. Recall the ODE for a 2D plane pendulum

$$\ddot{\theta} = -\sin \theta$$

and the ODEs for a 3D pendulum

$$\begin{aligned}
\ddot{\theta} &= -\sin \theta + \dot{\phi}^2 \sin \theta \cos \theta \\
\ddot{\phi} &= -2\dot{\theta} \dot{\phi} \cos \theta / \sin \theta.
\end{aligned} \tag{22}$$

Compare them with the ODE (21) (remembering that the meanings of  $\theta$  in (21) and in the ODEs for the pendulums differ in  $\pi$ ). When the top has no spin and no precession, it oscillates like a pendulum on a swivel suspension - just as the "rolling disk" without rolling! - "not noticing" presence of the horizontal surface.

## Equations in the software

(Script file *general.scr*)

The notation is

$V_{eff}$	Veff
$E'$	E1
$\alpha$	alf
$\beta$	bet
$\frac{aI_1}{I_3}$	ai1di3

### Constants

```

Pi = 3.141592653589793238462643
p5 = Pi/5
R = 1
Mg = 10
i1 = 5
i3 = 1
h = 2 {distance to the center of mass (l in equations)}
w3 = 20
te0 = 0.01
te10 = 0.1
coste0 = cos(te0)
sin2te0 = sin(te0)^2
fi10 = 0.1
a = i3*w3/i1
b = fi10*sin2te0 + a*coste0
ai1di3 = a*i1/i3
Veff = 0.5*i1*(b - a*coste0)^2/sin2te0 + Mg*h*coste0
E1 = 0.5*i1*te10^2 + Veff
alf = 2*E1/i1
bet = 2*Mg*h/i1

```

### Auxiliary variables

```

cosfi = cos(fi)
sinfi = sin(fi)
cospsi = cos(psi)
sinpsi = sin(psi)
coste = cos(te)
sinte = sin(te)
sin2te = sinte^2
sin3te = sinte*sin2te
fi1 = (b - a*coste)/sin2te
xc = h*sinte*sinfi
yc = - h*sinte*cosfi
zc = h*coste
sinficoste = sinfi*coste
cosficoste = cosfi*coste
cospsi2 = cos(psi + p5*2)
sinpsi2 = sin(psi + p5*2)
. . . . .
cospsi8 = cos(psi + p5*8)
sinpsi8 = sin(psi + p5*8)
x0 = xc + R*( cosfi*cospsi - sinficoste*sinpsi )
y0 = yc + R*( sinfi*cospsi + cosficoste*sinpsi )
z0 = zc + R* sinpsi*sinte
. . . . .
x8 = xc + R*( cosfi*cospsi8 - sinficoste*sinpsi8 )
y8 = yc + R*( sinfi*cospsi8 + cosficoste*sinpsi8 )
z8 = zc + R* sinpsi8*sinte
x10 = xc
y10 = yc
z10 = zc
x11 = 0
y11 = 0
z11 = 0 {Pivot}
x12 = 2*xc
y12 = 2*yc
z12 = 2*zc

```

## ODEs

```

t' = 1
te' = tel
tel' = 0.5*bet*sinte + (a*coste - b)*(a - b*coste)/sin3te
fi' = fi1
psi' = ai1di3 - coste*fi1

```

## Heavy top as a pendulum with spin

First play with a couple of a general setting of the initial values.

Load and play script files *w18.scr* and *general.scr*.

In this subsection we are going to demonstrate that the heavy top behaves approximately as a mathematical pendulum whose plane of oscillation declines from the vertical because the effect of spinning.

### Pure pendulum.

Observe that if we set spin  $\omega_3 = 0$ , then  $a = 0$ . With that in mind and recalling formulas (19), the ODEs (21) for heavy top simplify

$$\begin{aligned}\ddot{\theta}|_{a=0} &= \frac{\beta}{2} \sin \theta + \frac{b^2 \cos \theta}{\sin^3 \theta} = \frac{\beta}{2} \sin \theta + \dot{\phi}^2 \cos \theta \sin \theta; \\ \ddot{\phi}|_{a=0} &= \left( \frac{b - a \cos \theta}{\sin^2 \theta} \right)'_{a=0} = -2\dot{\theta}\dot{\phi} \cos \theta / \sin \theta.\end{aligned}$$

In the case when  $\dot{\phi} \equiv 0$  the first ODE here is similar to that for the 2D pendulum. Otherwise these system are similar to the ODEs (22) for 3D pendulum. Let us see this in action.

First - a top behaving like a 2D pendulum.

Load the script file *TopLikePendulum.scr* in which  $\omega_3 = 0$ ,  $\theta = 0.1$  (rad)<sup>8</sup> and  $\dot{\phi} = 0$ . Play it and observe that the body oscillates as a conventional mathematical pendulum. Load the scripts *TopLikePendulum0001.scr* where  $\theta = 0.0001$  so that the gap in the circumference is not even visible.

For a comparison, load from the subfolder *2D3Dpendulums* the script file *Pendulum2D.scr* of the real mathematical pendulum.

There you may change the initial values in the Constants from  $\dot{\theta} = 0$  to say  $\dot{\theta} = 1$  (meaning a some push to the pendulum). As a result, the pendulum would rotate in the vertical plane (rather than oscillate), and so would also the heavy top!

Let's play with the 3D simulations. First load from the folder HeavyTop the script file *PendulumApple.scr* where we set  $\dot{\phi} = 0.5$ , which initiates precession outlining an apple during the pendulum-like oscillation. That was for the heavy top. Now try the script file *PendulumApple.scr* with the same name from the subfolder *2D3Dpendulums*, which displays the same apple-shaped outline made by the mathematical pendulum.

**Remark 9** *The heavy top moves exactly like a mathematical pendulum only when  $\omega_3 = 0$  (no spin). Then, just as a mathematical pendulum depending*

<sup>8</sup>We cannot start with  $\theta = 0$  in ODEs for  $\ddot{\theta}$  because of singularity in those ODE for  $\theta = 0$  (and  $\theta = \pi$ ). The ODEs in  $u$  (for  $\theta = 0, \pi$ ) have singularity at  $u = \pm 1$ . In addition, the formula for  $V_{eff}$  (used in both versions of the ODEs) still contains the singularity at  $\theta = 0$ . See the section "Sleeping top" for more details.

In ODEs for  $\ddot{\theta}$  however we can sometimes bypass the point  $\theta = \pi$  which may be achieved only if  $\omega_3 = 0$  (no spin).

on the initial values of  $\theta$  and  $\dot{\theta}$ , the top may perform  $2\pi$  rotation (rather than oscillation) passing through the lowest point  $\theta = \pi$ .

**Remark 10** Of the two systems (20) in  $\ddot{u}$  and (21) in  $\ddot{\theta}$ , only the system in  $\theta$  properly simulates variation of  $\theta$  within  $[0, 2\pi]$  due to integration of  $\theta$ . On the contrary, the  $\ddot{u}$  system (20) hides  $\theta$  integrating  $u = \cos \theta$  instead, and attempts to retrieve  $\theta$  via  $\arccos$  cannot return  $\theta \in [0, 2\pi]$ . We see a strange effect running the script `u2w0HalfArc.scr`. In it  $\omega_3 = 0$  and the pendulum-like motion must pass through  $\theta = \pi$  towards  $2\pi$ , but bounces back instead. Moreover, at  $\theta = \pi$  (or  $u^2 = 1$ ) computer integration of both systems may halt with an exception because of division by  $\sin \theta$  in the system (21) or because of singularity in  $\sqrt{1 - u^2}$  in the system (20). The integration, however, may sometimes quietly pass over such points when the finite step is big enough.

Let's play with a few more heavy tops behaving like a pendulum.

Try `u2w001.scr` in which (unlike in `u2HalfArc.scr`),  $\omega_3 = 0.001$ . Yet even this negligibly small spin deflects the plane of oscillation from the vertical - therefore avoiding the point  $u = -1$  ( $\theta = \pi$ ).

## Effect of the spin.

The spinning heavy top however behaves differently. When it falls down under the force of gravity from the upper position, the vector of the reaction - the gyroscopic force - is perpendicular to the trajectory of the fall having nonzero components directed horizontally and vertically. The horizontal component pushes the spinning top into a precession, while the vertical component, pushing the top upward, overcomes the gravity at the lowest positions of the heavy top. Let us introduce some spin and watch how the growing values of the spin affect the pendulum-like behavior of the heavy top.

We are going to try one by one the files `Pendulumw1.scr`, then `Pendulumw5.scr`, `Pendulumw10.scr` and `Pendulumw20.scr` where only the case for `w1` ( $\omega_3 = 1$ ) looks like a pendulum outlining an apple with a gap below. Observe how this gap widens with growing  $\omega_3 = 5, 10, 20$ , and the motion does not resemble pendulum outlining an apple any more (the velocities are incompatible in these simulations).

Begin with smallest spin  $\omega_3 = 1$  loading and playing the script file `Pendulumw1.scr`. The axis point still outlines an apple shape, however now we see an "opening" in the bottom never reached by the axis. The oscillation takes place in (so far) a large strip constrained by two circumferences.

Now try the spin  $\omega_3 = 10$  loading and playing the script file `Pendulumw10.scr`. This time the oscillation takes place in a narrow strip constrained by two circumferences: the bigger is the spin, the bigger is the vertical component of the gyroscopic reaction acting against the gravity.

## The three cases

Subfolder *3Cases*.

Here we are to demonstrate (following the reports by Chloe Elliott [9]) that the motion of the heavy top is really contained within a particular strip  $\theta \in [\theta_{\min}, \theta_{\max}]$ . There are three types of the motion displayed via the trajectories of the tip of the rotation axis (Fig. 4):

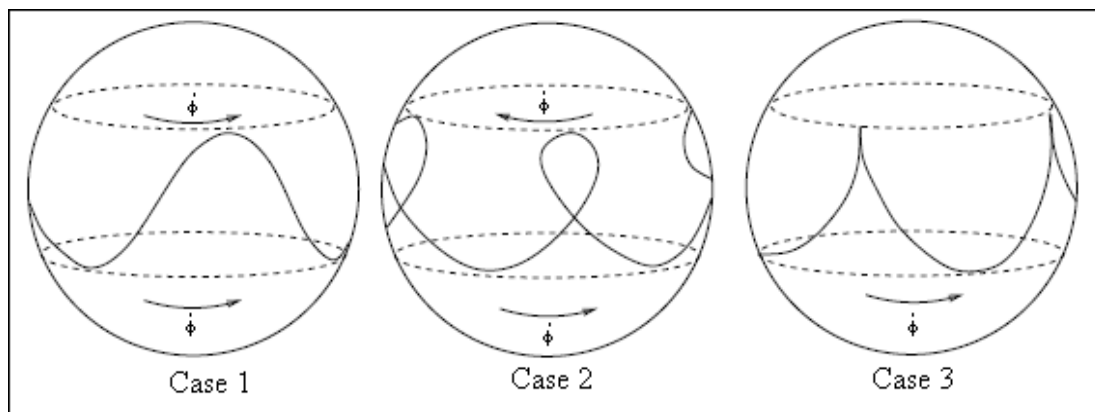


Fig. 4 Three types of motion (Fig. 44 in [9])

Actual width of the strip  $[\theta_{\min}, \theta_{\max}]$  may differ, and the wave length of the curve may be any, even several times longer than  $2\pi$ .

The analysis of the cases is based on the properties of the polynomial  $f(u)$  (18): in particular on its roots  $u_1, u_2$ , where

$$\begin{aligned} -1 < u_1 \leq u_2 < 1, \\ \theta_{\min} = \arccos u_1, \quad \theta_{\max} = \arccos u_2. \end{aligned}$$

Load the script file `fu.scr` displaying a graph for a sample of a cubic polynomial (in black) crossing the orange abscissa at the root points  $u_1, u_2$ .

**Case 1**  $\dot{\phi} > 0$  at both points  $u_1, u_2$ . Load script file `Case11.scr` where the red curve represents the arc of  $f(u) \geq 0$  crossing the abscissa at the points  $u_1, u_2$ , while the black curve  $\{u, f_{101}\}$  is  $\dot{\phi}(u) > 0$ . Now load and play the script file `Case1.scr` representing the actual motion corresponding to the Case 1.

**Case 2**  $\dot{\phi}(u_1) > 0$ , while  $\dot{\phi}(u_2) < 0$ . Load script file `Case21.scr` where the red curve represents the arc of  $f(u) \geq 0$  crossing the abscissa at the points  $u_1, u_2$ , while the black curve  $\{u, f_{101}\}$  is  $\dot{\phi}(u)$  as it should be in this case. Now load and play the script file `Case2.scr` representing the actual motion corresponding to the Case 2.

**Case 3**  $\dot{\phi}(u_1) > 0$ , while  $\dot{\phi}(u_2) = 0$ . Load script file Case31.scr where the red curve represents the arc of  $f(u) \geq 0$  crossing the abscissa at the points  $u_1, u_2$ , while the black curve  $\{u, f_{101}\}$  is  $\dot{\phi}(u)$  as it should be in this case. Now load and play the script file Case3.scr representing the actual motion corresponding to the Case 3.

## Uniform motion

The uniform motion of the heavy top is such when  $\theta = const$  (so that also  $u = \cos(\theta) = const$ ),  $\dot{\phi} = const$ , and  $\dot{\psi} = const$ . As it follows from the ODEs (21), if we obtain the solution  $\theta = const$ ,  $\dot{\phi}$  and  $\dot{\psi}$  are constants automatically. Our goal here is to demonstrate, that for any given tilt  $\theta$  of the top and for any big enough spin  $\omega_3$  it is possible to obtain the initial values of  $\dot{\phi}$  (and  $\dot{\psi}$ ) effectuating the uniform motion.

In the system (21) the ODE for  $\dot{\phi}$  does not help to obtain the required constant values of  $\dot{\phi}$ , but we are going to use the ODE (18) for  $u$  for that purpose. Though (18) does not visibly contain  $\dot{\phi}$ ,  $\dot{\phi}$  is present in ODE (18) implicitly via the constant relations (19).

$$b = \frac{p\dot{\phi}}{I_1} = \dot{\phi} \sin^2 \theta + a \cos \theta = \dot{\phi}(1 - u^2) + au$$

$$b - au = \dot{\phi}(1 - u^2).$$

With that in mind, let's deal with the ODE (18) with the goal to finally extract of it the condition for  $\dot{\phi}$ .

In order to achieve the uniform motion, we need that  $\theta_{\min} = \theta_{\max}$  which takes place when the roots  $u_1 = u_2$  in  $f(u) = 0$ . The condition for  $u_1$  to be a double root is that  $f(u_1) = f'(u_1) = 0$ .

$$f(u) = (1 - u^2)(\alpha - \beta u) - (b - au)^2 = 0$$

$$f'(u) = -2u(\alpha - \beta u) - \beta(1 - u^2) + 2a(b - au) = 0.$$

From the first one it follows that

$$(1 - u^2)(\alpha - \beta u) = (b - au)^2 = \dot{\phi}^2(1 - u^2)^2$$

$$\alpha - \beta u = \dot{\phi}^2(1 - u^2).$$

Now transform the second one:

$$-2u(\alpha - \beta u) - \beta(1 - u^2) + 2a(b - au)$$

$$= -2u\dot{\phi}^2(1 - u^2) - \beta(1 - u^2) + 2a\dot{\phi}(1 - u^2) = 0.$$

After ridding of  $(1 - u^2)$ , we get a square equation for  $\dot{\phi}$

$$u\dot{\phi}^2 - a\dot{\phi} + \frac{\beta}{2} = 0$$

whose solutions are

$$\dot{\phi}_{1,2} = \frac{a \pm \sqrt{a^2 - 2\beta u}}{2u}. \quad (23)$$

These solution are real (physical) if

$$a^2 - 2\beta u = \left( \frac{I_3 \omega_3}{I_1} \right)^2 - \frac{4Mgl u}{I_1} \geq 0$$

so that

$$\omega_3 \geq \frac{2}{I_3} \sqrt{Mgl I_1 \cos \theta} = \omega_{thresh}(\theta) \quad (24)$$

presenting the condition how big  $\omega_3$  must be for the given tilt  $\theta$  in order that the uniform motion take place with the two possible values  $\dot{\phi}_{1,2}$  of the precession of the top. Both solutions  $\dot{\phi}_{1,2}$  are of the same sign. They are known as the "slow" and "fast" precessions.

If  $\omega_3 \geq \omega_{thresh}(\theta)$  and  $\omega_3 \approx \omega_{thresh}(\theta)$  so that  $a^2 - 2\beta u \approx 0$ , then both  $\dot{\phi}_{1,2}$  are approximately the same and

$$\dot{\phi}_{1,2} \approx \frac{a}{2u} = \frac{I_3 \omega_3}{2u I_1} = \frac{I_3}{2u I_1} \frac{2}{I_3} \sqrt{Mgl I_1 \cos \theta} = \sqrt{\frac{Mgl}{I_1 \cos \theta}} \quad (25)$$

**Remark 11** For a given  $\theta$ , if  $\omega_3 < \omega_{thresh}(\theta)$ , the uniform motion is impossible for such  $\omega_3$  turning into one of the three non-uniform cases presented above.

**Remark 12** For a given  $\theta$ , if  $\omega_3 > \omega_{thresh}(\theta)$ , for such  $\omega_3$  there do exist two  $\dot{\phi}_{1,2}$  effectuating the slow and fast uniform motions.

**Remark 13** In both slow and fast uniform motion the axis moves along the direct circular cone so that the center of mass follows a circumference with the same radius  $r$ . For the bigger of the two  $\dot{\phi}_{1,2}$  the centrifugal force  $\dot{\phi}^2 r$  is bigger. In particular, if  $\dot{\phi}_2 > \dot{\phi}_1$  then

$$\text{Centrifugal}|_{\dot{\phi}_2} > \text{Centrifugal}|_{\dot{\phi}_1},$$

its  $z$ -projections for the same cone

$$\text{Centrifugal}_z|_{\dot{\phi}_2} > \text{Centrifugal}_z|_{\dot{\phi}_1}$$

acting down and adding to the gravity, so that the following balance of forces must take place:

$$(\text{Gyroscopic}_z - \text{Centrifugal}_z - \text{Gravity})|_{\dot{\phi}_1} = (\text{Gyroscopic}_z - \text{Centrifugal}_z - \text{Gravity})|_{\dot{\phi}_2} = 0$$

or

$$(\text{Gyroscopic}_z - \text{Centrifugal}_z)|_{\dot{\phi}_1} = (\text{Gyroscopic}_z - \text{Centrifugal}_z)|_{\dot{\phi}_2}$$

- compare with the formulas (9), (10) for the rolling disk.

Here are the formulas in the section *Constants* implementing these cases of uniform motion.

```

Pi = 3.141592653589793238462643
p5 = Pi/5
R = 1
Mg = 10
i1 = 5
i3 = 1
h = 2
w3 = 25
te0 = 0.3
te10 = 0
coste0 = cos(te0)
sin2te0 = sin(te0)^2
a = i3*w3/i1
u0 = coste0
bet = 2*Mg*h/i1
determ = a^2 - 2*bet*u0    {must be >0}
fi10 = 0.5*(a + sqrt(determ))/u0
b = fi10*sin2te0 + a*coste0
ai1iz = a*i1/i3
Veff = 0.5*i1*(b - a*coste0)^2/sin2te0 + Mg*h*coste0
E1 = 0.5*i1*te10^2 + Veff
alf = 2*E1/i1

```

## Simulations of the uniform motion.

Subfolder *HeavyTop\Uniform*.

First explore the function  $f(u)$  by loading the script file *w5fu.scr* and observing that the the curve touches the abscissa (as it should in this case).

There are two versions of the simulations for the two values  $\theta = 0.3, 1$  (radians): for each of them the fast precession version with "Plus" in the name corresponds to "+" in (23) and the slow version with "Minus" in the name corresponds to "-" in (23).

Load and play script files mentioned in the table below.

With all other constants as they are...

Script file	$\theta$	$\min \omega_3$	$\omega_3$	$\dot{\phi}$
<i>w20Minus03rad.scr</i>	0.3	19.54	20	1.65
<i>w20Plus03rad.scr</i>	0.3	19.54	20	2.53
<i>w15Minus1rad.scr</i>	1	14.7	15	2.22
<i>w15Plus1rad.scr</i>	1	14.7	15	2.22
<i>w25Minus1rad.scr</i>	1	14.7	25	0.88
<i>w25Plus1rad.scr</i>	1	14.7	25	8.37

## Discussion.

Here too it's instructive to analyze the cases of the uniform motion presented above *qualitatively*.

The center of the mass of the top moves along a circumference generating a centrifugal force whose component tends to overturn the top *together* with the gravity (unlike in the case of rolling disk). Here the only reaction acting upward counteracting the fall of the top is the gyroscopic reaction.

## The sleeping top

Subfolder *HeavyTop\Sleeping*

The term *sleeping top* is used for the heavy top whose axis is exactly vertical so that the top spins without nutation i.e.  $\theta = \dot{\theta} = 0$ ,  $u = 1$ ,  $b = a = \frac{I_3\omega_3}{I_1}$ ,  $\alpha = \beta = \frac{2Mgl}{I_1}$ ,  $\phi$  is not defined,  $\dot{\psi} = \omega_3 = \text{const.}$

Physically this case would not need a special consideration being merely a special case among those covered in the sections "Heavy top as a pendulum with spin" and "Three cases" when  $\theta_{\min} \approx \theta_{\max} \approx 0$ . Mathematically, however, we confront a problem that both systems of ODEs presented here for modelling the heavy top (17), (21) in general position are singular at  $\theta = \dot{\theta} = 0$ . We do not know if the systems of ODEs in  $u, \phi, \psi$  or in  $\theta, \phi, \psi$  modelling the general heavy top and regular for  $\theta = \dot{\theta} = 0$  even exist. The regular ODE (20) for  $u$  alone does exist and can be integrated as a stand alone ODE - but not together with the system (20).

In order to integrate a system specifically modelling the sleeping top, we must modify (regularize) the system (20) deliberately setting  $\dot{\phi} \equiv 0$  and computing the  $\lim_{\theta \rightarrow 0} V_{eff}$

$$\begin{aligned} V_{eff} &= \frac{I_1(b - a \cos \theta)^2}{2 \sin^2 \theta} + Mgl \cos \theta = \frac{I_1 a (1 - \cos \theta)^2}{2 \sin^2 \theta} + Mgl \cos \theta = \\ &= \frac{I_1 a (1 - u)^2}{2(1 - u^2)} + Mglu = \frac{I_1 a (1 - u)}{2(1 + u)} + Mglu; \\ \lim_{\theta \rightarrow 0} V_{eff} &= \lim_{u \rightarrow 1} V_{eff} = Mgl \quad (\text{valid only for } \theta|_{t=0} = 0). \end{aligned}$$

Moreover, for these specific initial values the the special solution may be expressed explicitly:

$$\begin{aligned} u &\equiv 1 \\ \theta &\equiv 0 \\ \phi &\equiv 0 \\ \dot{\psi} &= \omega_3. \end{aligned} \tag{26}$$

**Remark 14** *Though the special solution (26) does simulate the heavy top in the sleeping mode, it has little to do with its physical behavior and stability in this mode. In order to numerically explore and experiment with its stability, we must consider the general ODEs (21) simulating the heavy top with initial values  $\theta \approx 0$  (yet taking care that  $\theta \neq 0$ ).*

**Remark 15** *It's worth noting the distinction between this special solution (26) and the special solution for the Dzhanibekov effect. The solution corresponding to the Dzhanibekov effect is a regular solution of the respective system (11) for the free top, though unstable, while the sleeping top solution (26) makes the systems (20), (21) singular.*

The script file *ValidOnlyForte0.scr* demonstrates this special case.

In order to explore the stability of the sleeping top depending on its spin  $\omega_3$ , lets follow the approach by Chloe Elliott in [9].

He considers a modified ODE  $\dot{u}^2 = f(u)$  (18) under the special conditions  $a = b$  and  $\alpha = \beta$  (taking place for the sleeping top) so that in a new variable  $v$  it is

$$v^2 = f(v) = (1 - v)^2(\alpha(1 + v) - a^2). \quad (27)$$

The general solutions  $v(t; t_0) = u(t; t_0)$  only for the initial value  $v|_{t=0} = u|_{t=0} = 0$ : otherwise,  $v(t)$  is merely some approximation of  $u(t)$ . Observe that  $f(v) = (1 - v)^2(\alpha(1 + v) - a^2)$  has a double root  $v_1 = 1$  and another root from the condition  $\alpha(1 + v) - a^2 = 0$  or  $v_2 = \frac{a^2}{\alpha} - 1 = \left(\frac{I_3\omega_3}{I_1}\right)^2 / \left(\frac{2Mgl}{I_1}\right) - 1 = \frac{I_3^2\omega_3^2}{2I_1Mgl} - 1$ .

At the point of double root  $v_1 = 1$  the cubic curve  $f(v)$  may touch the abscissa in two different ways:

1.  $f(v)$  reaches its zero-maximum at  $v_1 = 1$  (staying below the abscissa) so that the root  $v_2 > v_1 = 1$ . Load the script *fuCase1.scr* to see this picture. Elliott defines this case as stable [9].
2.  $f(v)$  reaches its zero-minimum at  $v_1 = 1$  (staying above the abscissa) so that the root  $v_2 < v_1 = 1$ . Load the script *fuCase2.scr* to see the picture. Elliott defines this case as unstable [9].

**Criterion 1** *In terms of the spin  $\omega_3$ , stability of the sleeping top (when the root  $v_2 > 1$ ) means that*

$$\begin{aligned} \frac{I_3^2\omega_3^2}{2I_1Mgl} - 1 &> 1, \quad \frac{I_3^2\omega_3^2}{2I_1Mgl} > 2, \quad \omega_3^2 > \frac{4I_1Mgl}{I_3^2}, \\ \omega_3 &> \frac{2\sqrt{I_1Mgl}}{I_3} = \omega_{crit} \end{aligned} \quad (28)$$

*and respectively instability of the sleeping top (when the root  $v_2 < 1$ ) means that*

$$\omega_3 < \omega_{crit}.$$

**Remark 16** *It's interesting that the critical value  $\omega_{crit}$  here equals to the critical value (24) computed with  $\theta = 0$  (as obtained in the study of the uniform motion of the heavy top). The value (24) sets the low limit for  $\omega_3$  at which the uniform motion is possible for the given tilt  $\theta$ : for the sleeping top  $\theta \approx 0$ . Then, if  $\omega_3 < \omega_{crit}$ , the uniform motion is impossible, and the top will escape from the near vertical position similarly to a pendulum. Otherwise, if  $\omega_3 > \omega_{crit}$ , the top will move closely around the vertical in a manner depending on the initial  $\phi$ . If  $\dot{\phi} = 0$ , the motion will be chaotic, however if the  $\dot{\phi}$  is computed according to the formula (24) for the uniform motion, the axis uniformly follows the direct cone along a circle.*

In the real world, due to friction, the vertical top initially spinning fast with  $\omega_3 > \omega_{crit}$ , finally loses its velocity  $\omega_3$  so that it becomes  $< \omega_{crit}$  causing the top tilt more and more until it falls.

**Summary 1** *The following comparison Table summarizes the condition of uniform motion for the three cases considered in the previous sections:*

Uniform motion of...	$\theta$	$L_3, \omega_3$	$\dot{\psi}$	
Disk	$\theta \in (0, \frac{\pi}{2})$	$L_3, \omega_3 > 0$	$\dot{\psi} > \dot{\psi}_{thresh}$	$\dot{\phi}_{1,2}$ (6)
Top	$\theta \in (0, \frac{\pi}{2})$	$\omega_3 \geq \omega_{thresh}$		$\dot{\phi}_{1,2}$ (24)
Stable sleeping top	$\theta = 0$	$\omega_3 > \omega_{crit}$		(28)

## Discussion

It's instructive to compare numerical exploration of the Dzhanibekov effect for the free top with this case of the sleeping heavy top.

In the case of the Dzhanibekov effect we could integrate the ODEs exactly at the special points of interest  $\theta = \pi/2$ ,  $\psi = k\pi$  exploring the behavior of the solutions in the vicinity of those points.

On the contrary, in the case of the sleeping top, we cannot start at the point of interest  $\theta = 0$  exactly - because the available ODEs of the process are singular at  $\theta = 0$ . We can start however in the close neighborhood of  $\theta = 0$  comparing the actual numeric behavior with the estimates suggested by Chloe Elliott in [9].

Now play several simulations from the subfolder *Sleeping*.

In the following series of simulations the tilt  $\theta = 0.01$  (radians) and  $\omega_{crit} = 20$  (computed in accordance with (28)).

Script file	$\omega_3$	$\dot{\phi}$			Trajectory of axis:
<i>te01w25vs20.scr</i>	25	0		$\omega_3 > \omega_{crit}$	compact near the vertical
<i>te01w25vs20f1Uniform.scr</i>	25	1	(23)	$\omega_3 > \omega_{crit}$	small circle 0.01 radius
<i>te01w25vs20f4Uniform.scr</i>	25	4	(23)	$\omega_3 > \omega_{crit}$	small circle 0.01 radius
<i>te01w15vs20.scr</i>	15	0		$\omega_3 < \omega_{crit}$	escapes away from vertical
<i>te01w20vs20fi0.scr</i>	20	0		$\omega_3 = \omega_{crit}$	less compact near vertical
<i>te01w20vs20fUniform.scr</i>	20	2	(25)	$\omega_3 = \omega_{crit}$	small circle 0.01 radius.

In the cases of  $\omega_3 = 25$  and  $\omega_3 = 15$  we see a clear confirmation of the role of the Elliott's critical value (28) when  $\omega_3$  is far away from it. At that, when we set the right values of  $\dot{\phi}$  in accordance with (23), the axis trajectory becomes exactly circular of 0.01 radius. For  $\omega_3 = 15 < 20$  the circular motion is impossible.

For  $\omega_3 = 20$  it is still possible to set the right values of  $\dot{\phi}$  in accordance with (23), (25).

There are also other script files for the ODEs in  $\ddot{u}$  with  $\theta$  closer to the vertical, whose naming mnemonic reflects the same logic.

**Acknowledgement 1** *I am very thankful to Dmitry Garanin for attracting my attention to this topic and providing his manuscript [2]. And I am also thankful to Mark Ashbaugh for the communication and interesting ideas expressed in it.*

## References

1. The Taylor center software <http://taylorcenter.org/Gofen/TaylorMethod.htm>
2. Dmitry Garanin. "Rotational motion of rigid bodies". 2004, [http://lehman.edu/faculty/dgaranin/Mechanics/Mechanis\\_of\\_rigid\\_bodies.pdf](http://lehman.edu/faculty/dgaranin/Mechanics/Mechanis_of_rigid_bodies.pdf)
3. Euler's equations (rigid body dynamics), [https://en.wikipedia.org/wiki/Euler%27s\\_equations\\_\(rigid\\_body\\_dynamics\)](https://en.wikipedia.org/wiki/Euler%27s_equations_(rigid_body_dynamics))
4. [https://en.wikipedia.org/wiki/Rigid\\_body\\_dynamics](https://en.wikipedia.org/wiki/Rigid_body_dynamics) .
5. Euler disk [https://en.wikipedia.org/wiki/Euler%27s\\_Disk](https://en.wikipedia.org/wiki/Euler%27s_Disk)
6. Dzhanibekov effect video: [https://youtube.com/watch?v=1VPfZ\\_XzisU&t=0s](https://youtube.com/watch?v=1VPfZ_XzisU&t=0s), [https://en.wikipedia.org/wiki/Tennis\\_racket\\_theorem](https://en.wikipedia.org/wiki/Tennis_racket_theorem)
7. Mark Ashbaugh, Carmen Chicone, Richard Cushman. The twisting Tennis Racket. Journal of Dynamic and Differential Equations, Vol. 3 No. 1, 1991.
8. Louis Poinsot, Théorie Nouvelle De La Rotation Des Corps, 1851
9. Chloe Elliott. The Spinning Top, 2009, <https://damtp.cam.ac.uk/user/tong/dynamics/three.pdf>, or [https://maths.dur.ac.uk/Ug/projects/highlights/CM3/Elliott\\_Spinning\\_Top\\_report.pdf](https://maths.dur.ac.uk/Ug/projects/highlights/CM3/Elliott_Spinning_Top_report.pdf)

# Appendix

## The software basics and installation

A detailed outline of the Taylor Center software may be found here [1]. The hot link in [1] for downloading it is:

<http://taylorcenter.org/Gofen/TaylorCenterDemo.zip> .

Download and unzip the file ("*Save*", don't "*Open*" it in your browser). Unzip and keep it in an empty folder of your choice, *TCenter.exe* being the only executable to run. Preserve this file and sub-folders structure (in order that the program work properly).

Then download a zipped structure of folders with script files of the simulations from here

<http://taylorcenter.org/Exploratorium/RigidBody.zip>

and unzip it into an empty folder of your choice, say *RigidBody*. This will be your folder to navigate from the program *TCenter.exe* in order to pick the necessary script and the file *SimulationsCatalog.rtf* containing the list of all script files in this Exploratorium.

In the program you have to distinguish the *Main* (or *Front*) window, and the *Graph* window (which displays trajectories). Within the *Main* window there are 4 tabbed pages: *Equation setting*, *Debugging*, *Integration setting*, and *Graph setting*. When you load a script, you immediately get into the *Graph* window to play with the loaded simulation. However, in order to explore the ODEs and parameters, you will have to visit the tabbed pages of the *Main* window.

## 1 Methods of loading and playing scripts

Here are several methods of loading scripts (occurring inside the pdf file of this Exploratorium) with various levels of automation.

1. No automation (when the Exploratorium is on paper). This is a general case (unrelated to this Exploratorium) when you wish to load scripts from any folder, say, *Samples* coming with the Taylor Center software. With this method, in order to load a particular script file (say, mentioned in the *print*), go to *File/Load script* menu either in the *Main* or in *Graph* window, and navigate to the desired folder in the *open file* dialog box (the mode of displaying in the dialog box must be detailed list in alphabetical order). Examining this list, find the file mentioned in the Exploratorium. The moment you click *Open*, this file will be run displaying the final picture of the motion. Then, by clicking *Play* button, you can run the simulation and watch the motion in real-time. Most simulation are in 3D stereo (on a black background) requiring a pair of red/blue glasses. Clicking the check box *Axonometry*, you can view them conventionally without the red/blue glasses just as other 2D images.

2. For this and the following methods, first load the catalog of all simulations of this textbook under *Demo/Load script list* menu item in the main window. There, in the *Open file dialog box* navigate to your folder *RigidBody* and in it open the file *SimulationsCatalog.rtf* so that you will see the list of all available simulations in the *Help window*. You can run each of them by double clicking the desired file at any place of the line (instead of navigating inside all required sub-directories in Method 1).

More automation is available when this Exploratorium is a pdf file which you read at the same PC. While reading the pdf text from your screen, when you wish to run a particular simulation, first **select and copy the desired file name into the clipboard by your mouse**. This is a presumption for the Methods 3 and 4 below when the check box *Auto mode* is either unchecked, or checked

3. In the Help window the check box *Auto mode* is unchecked. Having the script file of interest already copied into the clipboard, just click over the Help window activating it - and this action will trigger running of the selected script in the clipboard.
4. In the Help window the check box *Auto mode* is checked, meaning that the Taylor Center is in auto mode keeping to check whether the clipboard has changed every half second. In this fully automatic mode, in order to run every script of your interest mentioned in the pdf file, all that you need is to select it in the pdf reader and copy it into the clipboard. In a matter of a second you will get this file loaded and ready for playing in the Taylor Center.

If you plan to compare graphs of some two related simulations, you may load two instances of the *TCenter.exe* (especially if having a wide screen or two monitors). Having the two instances of the program loaded, you may watch still images at both, however do not initiate *Playing* simultaneously, because the real-time playing function requires the entire resources of the PC exclusively.

After running a script from the Exploratorium, you may wish to make a change in the initial values and constants in order to see their effect. In order to do it, look into the editor panes for *Constants* and Initial values in the *Main* window, making the desired change. When a change is made, the Graph window disappears, and you need to *Compile* the modified problem. If the compilation succeeded (i.e. you did not introduce mistakes), you will see the *Graph* page. In it click the *Previous* button - which will bring you again to the Graph window ready to play the modified problem. After your changes, the *previous* setting of the sizes may happen to be not the best. Click the button *Adjust* which adjusts the sizes to create enough room for the image.

## The optimal conditions for stereo viewing

In order to perceive the real stereo, you need a pair of red/blue glasses (the left - red, the right - blue) putting them over your optical glasses used for reading screens. If you do not have red/blue glasses, you still can watch the simulations switching them into the mode of the conventional axonometric projection (the check-box Axonom).

In order to achieve the best stereo effect, the following setting should be made for your monitor and environment.

In a case of a desktop monitor here are the optimal settings...

1. Better have a monitor with black matte surface.
2. The light in the room must be as little as possible so that the surface of an inactive monitor look black.
3. Have a pair of Red/Blue glasses whose Red and Blue filters let through only the narrow spectrum of the respective colors. In order to test that your glasses satisfy this criterion, overlap two pairs of such glasses with the opposite filters over each other and look at the bright light. Ideally, the overlapped filters must let through no light at all so that a bright light source is hardly visible.
4. Set the Contrast of the monitor to the maximum value of 100.
5. Set the Brightness of the monitor as low as possible with such a goal that the black on the monitor look absolutely black (rather than pale gray). With modern high luminance monitors your brightness values may happen to be as low as 10.

In a case of a screen projector...

- The light in the room must be zero.
- Set the Contrast of the projector to the maximum value of 100.
- Set the Brightness of the projector as low as possible with such a goal that the black on the screen look absolutely black (rather than pale gray). Your brightness values may happen to be as low as 10.

Both for a desktop and a screen projector the goal of the best setting is such, that there be no ghost images visible, i.e. that the right eye see only the right image in blue and nothing in red, while the left eye see only the left image in red and nothing blue.